Stiffness-induced EMT and Cancer Stemness in Glioblastoma Using Polyacrylamide Hydrogels

Mohammed Moaadi A Alotaibi

(BEng)

Primary supervisor: Prof. Manuel Salmeron-Sanchez

Secondary supervisor: Dr Udesh Dhawan

Abstract

Gliomas are the most common type of brain and are considered one of the most fatal cancer forms due to their detrimental and aggressive behaviour. Amongst these types of brain cancer is glioblastoma (GBM), classified by the World Health Organization (WHO) as grade IV, known to have characteristics like high malignancy, rapid growth and aggressiveness. As these tumours progress, the extracellular matrix (ECM) stiffness increases, influencing their growth, survivability and treatment outcomes.

The induction of Epithelial to Mesenchymal transition (EMT) was associated with the production of Cancer stem-like cells (CSCs), a small subpopulation with self-renewal capabilities that generates phenotypic heterogeneity comparable to the original tumour. CSCs are responsible for sustaining tumour growth and metastasis formation to other body tissues.

The main focus of this study was assessing the role of brain tissue mechanical stiffness in promoting EMT and cancer of glioblastoma cells. The surface of PAAm hydrogels was modified to overcome the non-adhesiveness via covalently linked to collagen type I to facilitate the attachment of glioblastoma cells.

The stiffness of Polyacrylamide Hydrogels (PAAm hydrogels) was measured using Rheology and Nanoindentation. The three stiffnesses fabricated and used were soft 305.9±16.9 Pa, which is similar to normal brain tissue, medium 10.5±0.4 kPa, comparable to glioblastoma stiffness and rigid 34.9±5.1kPa which is stiffer than glioblastoma tumours. The nanoindentation measurements were for soft 321.72±59.83 Pa, medium 8.01±0.37kPa and rigid 39.19±2.58kPa, illustrating that the stiffnesses are unfirmed across the surface and reproducible.

EMT markers like N-CAD, VIMENTIN and TGF-β showed increased protein levels in the medium and rigid hydrogels compared to soft hydrogels. This response was further by increased protein expression of the EMT transcription factor SNAI1(SNAIL), which showed a significant increase in levels of SNAI1(SNAIL) ($p \leq 0.05$) on the medium and rigid hydrogels.

CSC markers showed increased protein levels highlighted by the significant increase in the protein levels of NESTIN ($P \leq 0.001$), CD133 ($P \leq 0.0001$), POU5F1(OCT-4) ($P \leq 0.05$), and EGFR ($P \leq 0.05$), respectively on the rigid hydrogels compared to soft hydrogels. Medium hydrogels showed significant increases in the protein levels of CD133 ($P \leq 0.0001$) and POU5F1(OCT-4) ($P \leq 0.05$), respectively.

The findings of this research suggest that mechanical stiffness promoted EMT and cancer stemness in glioblastoma cells, underlining the influence of microenvironment stiffness in promoting invasion capabilities in glioblastoma cells.

Table of Contents

List of Tables

List of Figures

Author's Declaration

I confirm that the work presented in this thesis is my own, and at the time of submission is not being considered for any other academic qualification. Where information has been derived from other sources, I confirm that this has been indicated in this thesis.

JUNE 2024

Abbreviations

Abbreviations	Full name
µL	Microliter
AAm	40% Acrylamide Solution
APS	Ammonium persulfate
BSA	Bovine serum Albumin
BisAAm	2% N`, N`- Methylenebisacrylamide
CSC	Cancer stem cell
DMEM	Dulbecco's modified Eagle's medium
DPBS	Dulbecco's phosphate-buffered saline
ECM	Extracellular matrix
EMT	Epithelial to mesenchymal transition
E-CAD	E-cadherin
FBS	Foetal bovine serum
FN	Fibronectin
GAPDH	glyceraldehyde 3-phosphate dehydrogenase
GBM	Glioblastoma
kPa	Kilopascal
MET	mesenchymal-epithelial transition
NaOH	sodium hydroxide
NFW	nuclease-free waster
N_2	Nitrogen
N-CAD	N-cadherin
Pa	Pascal
PAAm	Polyacrylamide Hydrogels
PVDF	Polyvinylidene difluoride
qRT-PCR	Quantitative Real-Time PCR
SDS-PAGE	sodium dodecyl sulfate–polyacrylamide gel electrophoresis
TBST	Tris-buffered saline containing 0.1% Tween-20
TEMED	N, N, N`, N`- Tetramethyl ethylenediamine
TME	Tumour microenvironment

1 Introduction

For many decades, diseases like cancer have been studied to develop new treatments or to gain a deeper understanding of how this disease develops. Cancer, like many other diseases, has many types, and among these, it has different grades indicating its severity and how far it has developed. This illustrates how complex a disease cancer is and how much it requires to be understood entirely; although it can be in one part of the body, it can have different types of cells, further adding to the complexity of cancer. In cancer, the risk of the disease is not only to the specific organ as it can spread throughout the body, making it one of the most challenging illnesses to study and treat.

1.1 Brain cancer (glioblastoma)

Malignant brain tumours are some of the most catastrophic types of tumours. Amongst them, gliomas are the most common type of brain cancer that accounts for over 80% of all primary brain malignancies (Ostrom et al., 2015). They are considered among the deadliest forms of human cancer due to their invasiveness, aggressiveness, and destructiveness (Maher et al., 2001). Glioma is any tumour originating from the glial brain cell, with three types of cells with tumour-producing potential. The first cell type is an ependymal cell, which gives rise to ependymomas, oligodendrocytes that form oligodendrogliomas; and lastly, astrocytes, which lead to astrocytoma and include glioblastoma (GBM). However, according to the World Health Organization (WHO), this classification has been rendered obsolete as brain tumours that are low-grade and high-grade. Low-grade tumours are split into two grades, the first being WHO Grade I, which is characterised as the least malignant, long-term survival and slow growth, and this grade includes pilocytic astrocytoma and ganglioglioma. The second low-grade tumour classification is WHO grade II, which includes pineocytoma and pure oligodendroglioma, which are relatively slow and may occur at higher grades. The high-grade tumours also have two grades, the first being WHO grade III, which has infiltrative characteristics and tends to recur as a higher grade; this grade includes anaplastic astrocytoma and anaplastic oligodendroglioma. Lastly, the second high-grade tumour is WHO grade IV, which has the following charismatics: rapid growth, rapid recurrence, necrosis prone, highly malignant, aggressive, and widely infiltrative. This grade includes GBM, which is the focus of this project. The annual

incidence rate of GBM is 4.6 per 100,000 in England (Brodbelt et al., 2015; McNamara et al., 2022). Despite treatment, GBM, in most cases, recures with a median overall survival of 14.6 months and below 10% have 5-year survival(Stupp et al., 2009).

1.2 Tumour microenvironment (TME)

The tumour microenvironment (TME) varies greatly between healthy and cancerous tissue, and this change heavily influences cell behaviour. Understanding the environment in which diseases develop can contribute to the development of new treatments. Previous studies have shown that as the disease progresses, the stiffness of the extracellular matrix (ECM) in glioma tumours increases, influencing cell behaviour (Sohrabi et al., 2023). Furthermore, the mechanical properties of the solid tumour, including GBM, influence their growth and treatment outcome (Bhargav et al., 2022; Deng et al., 2022). The ECM stiffens where GBM cells with a mesenchymal phenotype show altered ECM proteins, increasing the recurrence of GBM cells and facilitating their survival, growth, and innovation (Y. Kim & Kumar, 2014; Miroshnikova et al., 2016). The increased stiffness in the tumour ECM is due to the elevated production of proteins (e.g. Fibronectin) and polysaccharides (e.g. hyaluronic acid) (Chauvet et al., 2016; Mohiuddin & Wakimoto, 2021). Overall, previous studies have demonstrated the importance of mechanical stiffness in influencing tumour growth and treatment outcomes and why it should be considered in the development of new therapeutic strategies (Bhargav et al., 2022; Yui & Oudin, 2024).

1.3 The mechanical stiffness of GBM

Despite new therapies, invasion is still a significant challenge to cure GBM. It has been attained that there is a major role in the invasive capability played by the mechanical cue within the external tissue environment (Butcher et al., 2009; Grundy et al., 2016; Mouw et al., 2014; Paszek et al., 2005). It has been suggested in previous studies that GBM are stiffness sensitive as GBM cell invasion is inhibited on soft matrices like the brain tissue and increases as the matrix stiffness increases (S. N. Kim et al., 2014; Ulrich et al., 2009). However, this was contradicted by

new studies that have shown a stiffness-independent response of patient-derived GBM lines (Ruiz-Ontañon et al., 2013; Wong et al., 2015). This can be justified because GBM subclasses represent distinct molecular and genetic properties (Phillips et al., 2006; Verhaak et al., 2010), and the majority of commonly used GBM cell lines, including the one in the initial studies, are of mesenchymal subclass (Verhaak et al., 2010).

In GBM tumours, as in any other solid tumours, the tumour tissue expansion is offset by the matrix proteins secreted by the GBM, increasing the mechanical forces on the tumours (Mahesparan et al., 2003; Payne & Huang, 2013). Due to the rapid growth of GBM at the late progression stages of the disease, the mechanical forces are increased on the whole brain as the rigid skill prevents tissue expansion (Behin et al., 2003). As a result of the increased pressure and its resulting strain, the GBM and natural tissue ECM stiffen (Pogoda et al., 2014). It is important to note that migration of the glial cells is compromised on soft brain tissue and is greatly improved on the stiffened ECM due to strain (S. N. Kim et al., 2014). Therefore, increased mechanical forces and tumour stiffness are induced in the natural course of GBM progression. In normal brain ECM, stiffness ranges from 0.2 to 1.2 kPa, and during the development of GBM tumours, it increases up to 10 kPa (Barnes et al., 2017; Franze, 2013).

1.4 Epithelial to mesenchymal transition (EMT)

Epithelial-mesenchymal transition (EMT) is a process in which cells acquire increased motility, lose their epithelial characteristics like cell polarity and cell-cell junction, and gain mesenchymal properties (Choi et al., 2013; Hollier et al., 2009; Micalizzi et al., 2010). Due to EMT, the close contact between epithelial cells from finically polarised tissue is disrupted, and it is characterised by loss of apical-basal polarity, cell-cell adhesion, and the obtaining migratory properties producing mesenchymal cells that are loosely organised (Thiery et al., 2009). This is associated with changes in gene expression where epithelial markers (e.g. E-cadherin) are downregulated, and mesenchymal markers (e.g. vimentin) are upregulated (Zeisberg & Neilson, 2009). During the formation of secondary tumours and epithelial organs, the cells undergo the reverse of this process, mesenchymal-epithelial transition (MET)(Their, 2002). EMT has been noted in cancer at the invasive front of the tumour mass, which is involved in the

acquisition of the required motility needed for metastasis and invasion. After the tumour cells have circulated, the migratory cancer cells can establish secondary tumours by undergoing MET (Their, 2002; Thiery et al., 2009).

Many biological processes, including EMT, are directed via mechanical cues from the microenvironment (Gomez et al., 2010; Nelson et al., 2008). EMT markers have different responses due to stiffness depending on the type of cancer. In terms of GBM, there might not be any changes in the expression of E-cadherin as it is rarely expressed in GBM (Iwadate, 2016; Paul et al., 2013). In glioma, EMT is induced via different signals, starting with Twist, which is transcriptionally active during the linage determination and cell differentiation (Castanon & Baylies, 2002; M. H. Yang et al., 2008). Twist suppresses E-cadherin (E-CAD) and upregulates Fibronectin (FN) and N-cadherin (N-CAD) when cancer metastasises by EMT (M. H. Yang et al., 2008). In malignant gliomas, Twist is upregulated and promotes cell invasion, and when Twist expression is inhibited, stem cell sphere formation and growth are significantly reduced in GBM (Elias et al., 2005; Mikheeva et al., 2010; Nagaishi et al., 2012). A second inducer is Snail, a member of the SNAIL family of transcription factors and acts as a primary suppressor of E-cadherin and expression (Boutet et al., 2006; Kalluri & Weinberg, 2009; Zeisberg & Neilson, 2009). Another member of the SNAIL family is Slug, and in numerous cancer cells, Slug plays a major role in the suppression of epithelial phenotype (Kalluri & Weinberg, 2009; H. W. Yang et al., 2010; Zeisberg & Neilson, 2009). It is also closely associated with the increased migratory and invasive properties in malignant gliomas (Xie et al., 2012). ZEB family is another family of transcription factors closely associated with EMT mediation in numerous types of cancer (Kalluri & Weinberg, 2009; Q. Wang et al., 2014; Zeisberg & Neilson, 2009). ZEB also increases motility by binding to the promoter region of the E-cadherin and suppressing its expression, resulting in loss of cell-cell contact (Qi et al., 2012; Sánchez-Tilló et al., 2012).

1.5 Cancer stem-like cells (CSCs)

The term Cancer stem cell-like cells (CSCs) refers to a small subpopulation of cancer cells that drive tumour progression. They have two distinct abilities: self-renewal, which allows for unlimited division and ensures tumour growth, and the

generation of phenotypic heterogeneity similar to the original tumour (McDermott & Wicha, 2010). CSCs are implicated in sustaining the growth and initiating primary tumours, and they are responsible for the establishment of metastasis at distal sites (Abraham et al., 2005; Al-Hajj et al., 2003a; Ginestier et al., 2007; Liu et al., 2007; Sheridan et al., 2006). CSCs show chemoresistance and asymmetric cell division (Al-Hajj et al., 2003a; Bonnet & Dick, 1997; Gupta et al., 2009). It has been suggested that the increased levels of aldehyde dehydrogenase (ALDH) and the expression of adenosine triphosphate-binding cassette transporter (ABCG2) can be used to characterise CSCs (An & Ongkeko, 2009; Storms et al., 1999; Zenzmaier et al., 2008).

The subpopulation of $CD133^+$ cells was identified as CSCs in GBM due to their ability to reconstitute the heterogeneity of the original tumours (Hemmati et al., 2003; Singh et al., 2003). Another marker used for identifying the CSCs is NESTIN, which is a protein that is often used to detect neural stem cells that play an essential role in the maintenance and self-renewal of stem cells (Neradil & Veselska, 2015; Strojnik et al., 2007). Furthermore, the CSCs phenotype is described by the co-expression of NESTIN and with other stem cell markers (e.g. CD133)(H. Wang et al., 2009).

1.6 The association between EMT and CSCs

2013, a CSC plasticity model has been proposed where they can switch between CSC and non-CSC states, which is a dynamic ability controlled by intrinsic and extrinsic stimuli (Meacham & Morrison, 2013). This adds to the complexity of the heterogeneity of the tumour within tumours and the fact that EMT is a reversible and dynamic process, where complex transcription programs are implicated and mediated through transitional factors such as TWIST, SNAIL family and ZEB family, leading to the loss of cell-cell attachment and apical-basal polarity, the expression and reorganisation of cytoskeletal protein and degradation of the ECM resulting in the acquisition of mesenchymal traits facilitating the invasion, migration and metastasis (Kalluri, 2009; Lamouille et al., 2014; Nieto et al., 2016). Since EMT is a reversible process and has a hybrid state, it provides an advantage in promoting metastases where the question of mesenchymal traits allows the tumour cells to disseminate and invade while conserving epithelial features that can facilitate reprogramming them to an epithelial state that supports metastatic outgrowth (da

Silva-Diz et al., 2018; Gunasinghe et al., 2012; Ocaña et al., 2012). The induction of EMT, as well as providing the cell with the migratory and invasive potential, also enhances the tumour-initiating and self-renewal capabilities, leading to the expression of stem-cell markers, indicating EMT involvement in the production of CSCs (Mani et al., 2008; May et al., 2011; Scheel & Weinberg, 2012).

1.7 CSC and Drug Resistance

Chemoresistance is one of the main issues associated with cancer, particularly in GBM, where the tumour heterogeneity plays a major role as it hosts many types of cells, including CSCs that bestow the tumour with chemoresistance (Gupta et al., 2009). Furthermore, CSCs can elude conventional therapies by remaining dormant, manipulating the TME, and increasing DNA repair capacities (Y. Li et al., 2021; Steinbichler et al., 2018). Many markers have been proposed as CSC biomarkers, starting with CD133, a glycoprotein observed in human hematopoietic stem cells and neuro-epithelial stem cells in mice. CD133 expression has been found in many types of tumours as it is not restricted to normal stem cells, where the expression of CD133 was discovered in brain tumours and used to identify brain cancer (Dirks, 2008). CSCs expressing CD133 exhibit self-renewal capability, and over-expression has been associated with reduced overall survival and poor prognosis in several types of tumours (Y. Li et al., 2021; Yiming et al., 2015). A second CSC biomarker essential for spindle assembly cell-cycle progression is NESTIN, where the NESTIN deficient cells are more sensitive to microtubule destabilising drugs as it causes abnormal spindle formation (Q. Wang et al., 2021). Lastly, ALDH1 is a CSC biomarker associated with drug resistance, as ALDH1 activities are essential in detoxifying exogenous and endogenous aldehydes (Pors & Moreb, 2014). The detoxification process where ALDH1 detoxifies toxic aldehyde intermediates produced in cancer cells treated with specific therapeutic agents grants therapy resistance to $ALDH1^+$ cells (Raha et al., 2014).

1.8 Models to Study Cancer

1.8.1 Two-Dimensional cultures

2D cell cultures have been traditionally used for preclinical drug testing, where the first record was published by Harrison et al. in 1907 (Harrison et al., 1907). It

has many recognised advantages, such as well-documented protocols, low cost, and ease of observation, analysis, and cell processing. In terms of cancer research, prior to animal studies and human clinical trials, more than 70% has been conducted on 2D culture systems (Hutmacher, 2010). However, the repeated passage on rigid substrates can lead to a selective homogenous monolayer being formed that has rapid proliferation and an increased survival rate, which poorly represents the heterogeneity of the 3D population (Burdett et al., 2010). In terms of GBM co-cultures, which typically involve mixing GBM cells and the surrounding brain microenvironment, can include many types of cells, such as neurons, astrocytes, macrophages, oligodendrocytes and microglia. Where on 2D platforms, a combination of GBM cells and microenvironment cells are grown in contact on flat culture vessels as a monolayer (Kapałczyńska et al., 2018). Although 2D models have been well-established with regard to the characterisation of GBM cell phenotypes and drug screening throughput, there are several pivotal limitations, such as the occurrence of changes over time in morphology and phenotype, in addition likely due to the growth of the cells on a flat surface does not mimic their behaviour *in-vivo* and growth patterns the cell susceptibility to genetic drift phenomenon is increased (Melissaridou et al., 2019; Torsvik et al., 2014; Y. H. K. Yang et al., 2018).

1.8.2 Three-dimensional Cultures

In the 1970s, Hamburg and Salmon carried out one of the first 3D cultures made in soft agar solution; since then, cell-cultured under 3D conditions have been shown and documented to have fascinating similarities to tumour mass(Hamburger & Salmon, 1977; Mazzoleni et al., 2009; Pampaloni et al., 2007). This type of culture allows for accurate imitation of the architectures of the original tissue compared to 2D, resulting in more interaction between cell-cell and cell-environment, allowing for imitation of cell structure where the cell can be similarly stimulated via local environment to *in-vivo* (Cawkill & Eaglestone, 2007; Griffith & Swartz, 2006; J. Lee et al., 2008). Although 3D cultures have a more accurate representation of the microenvironment, they come with many challenges, as the culture formation time might take up to a few days, worse reproducibility and performance compared to 2D in addition to higher costs (Baker & Chen, 2012; Hickman et al., 2014; Krishnamurthy & Nör, 2013).

1.8.3 Polyacrylamide Hydrogels (PAAm)

Polyacrylamide hydrogels have been a favoured choice to study the interaction between the cells and mechanical substrate due to their easy application and utilisation (Beningo et al., 2002; Y. L. Wang & Pelham, 1998) (Fig.1). The use of these hydrogels provides multiple chemical, optical and mechanical advantages, as they can produce a linear deformation and a rapid, complete recovery in response to a wide range of stresses and removal of these stresses. Additionally, the stiffness of these hydrogels can be manipulated by varying the concentration of the bis-acrylamide cross-linker, which is a feature unique to these gels. These gels can facilitate visualisation via microscopy as they are non-fluorescent and clear. Moreover, the non-adhesive substrate surface can covalently link proteins of interest (Kandow et al., 2007).

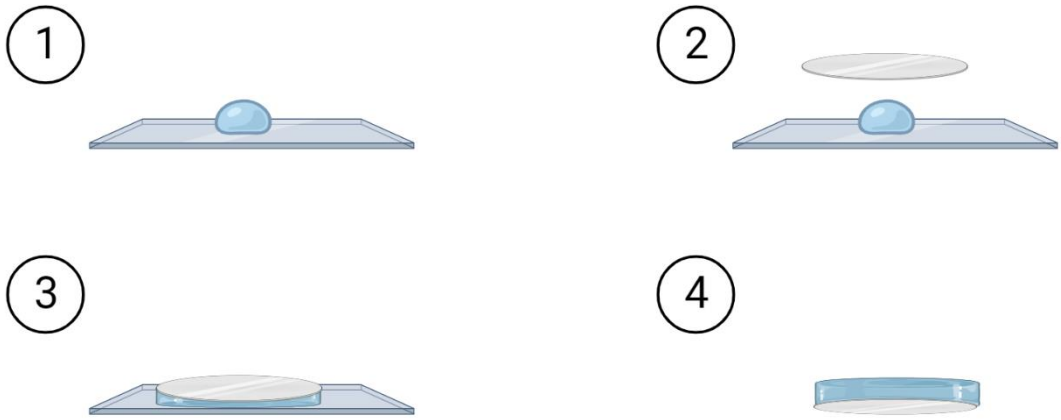

Figure 1. The procedure for making the PAAm hydrogels. A drop of the Activated solution is added to a nonreactive glass slide. A circular coverslip with a reactive surface that binds to the PAAm solution is overlaid onto the PAAm droplet. Following polymerisation, the coverslip with PAAm attached is carefully removed, then placed in water and stored at 4C° to swell overnight.

1.9 Aim and Objectives

The main aim of this thesis is to investigate the role of mechanical stiffness of brain tissue in inducing epithelial-mesenchymal transition (EMT) and cancer stemness in GBM cells. To achieve this aim, the following strategies were followed:

- Fabricate PAAm hydrogels of the desired stiffness and asses the uniformity of the stiffness across the surface.

- Conduct an *in-vitro* study to optimise and functionalise the PAAm hydrogels.

- Assess the response of the cell to different stiffness of PAAm hydrogel.

- Assess the influence of stiffness on EMT markers and CSC markers.

2 Materials and Methods

Experimental outline

The primary focus of these experiments, which holds significant implications for our understanding of GBM, was to assess whether primary human brain cancer cells from GBM (PAT1S) cultured on PAAm gels with different stiffnesses would have higher cancer stemness properties in a stiffness-dependent manner.

This chapter provides a comprehensive overview of the production and optimisation of the PAAm with different stiffness, evaluation of cellular response, investigation of EMT markers and CSC markers, and the microenvironment stiffness that influences them. It also covers optimising surface functionalisation and assessing whether the response is due to the ligand density or stiffness.

2.1 Materials

The following materials were used in the preparation and surface coating of the PAAm gels:

- Ammonium persulfate (APS). (Scientific Laboratory Supplies, Cat: A3678-25G).
- N, N, N`, N`- Tetramethyl ethylenediamine (TEMED) (SIGMA-ALDRICH, Cat: T9281)
- 40% Acrylamide Solution (AAm) (SIGMA-ALDRICH, Cat: A4058)
- 2% N`, N`- Methylenebisacrylamide (BisAAm) (SIGMA-ALDRICH, Cat: M1533)
- 3-(Acryloyloxy) propyltrimethoxysilane (ThermoScintific, cat: L16400.14)

- Sulfo-SANPAH (SIGMA-ALDRICH, Cat: 803332)
- rainX (rainX, ref: 26062)
- Collagen type 1, Rat Tail 100 mg (Corning Cat:354236)
- Glass slides
- Circular coverslips 12 mm,30 mm and 50 mm
- Glass block

2.2 Preparation of PAAm hydrogels

The preparation of the PAAm hydrogels was a meticulous process requiring a fume hood. The 12 mm coverslips were cleaned by sonicating twice in dd water for 30 min in dd water, followed by a 30 min sonication in ethanol and rinsed twice with dd water. The coverslips were then allowed to air dry for a few minutes. Then, the coverslips were acrylsailnised by submerging in a solution containing 50 mL ethanol, 2.5 mL di water and 231µL of 3-(Acryloyloxy) propyltrimethoxysilane (ThermoScintific, cat: L16400.14) for 1 h in a fume hood followed by tempering at 120 °C in a drying oven.

An intermediate concentration of TEMED at 1.5 % in di water was made by adding 8 µL of TEMED in 492 µL of di water and 5 % APS, where 20 mg was added to 380 µL of di water. The gels were prepared using the following concentration of the reagents:

Table 1. The PAAm gels component and amounts.

Reagent	Soft	Medium	Rigid
AAm	30 µL	50 µL	100 µL
BisAAm	12 µL	60 µL	60 µL
H_2O(di water)	325 µL	257 µL	207 µL

TEMED	25 µL	25 µL	25 µL
APS	8 µL	8 µL	8 µL

The glass slides were submerged in rainX for 5 min and then allowed to air dry; the amounts from Table 1 of AAm, BisAAm, and TEMED were mixed and vortexed. As soon as the APS was added, the mixture was immediately vortexed, and 10 µL of the mix was added on top of the glass slide and topped by the acrylsailnised 12 mm coverslip. The gels were then allowed to polymerise for 10 min, then lifted with tweezers and kept in dd water at 4 °C to swell overnight.

Table 2. The amount of PAAm gel mixture used for each coverslip size.

Coverslip size	Amount of PAAm gel mix
12 mm	10 µL
18 mm	15 µL
30 mm	25 µL
50 mm	100 µL

To make the 30mm and 50mm PAAm hydrogels, first, the coverslips were placed in a large petri dish, covered with 0.1M sodium hydroxide (NaOH) for 5 min, rinsed twice with dd water, and then washed with dd water on a shaker for 5min. The coverslips were dried under N_2 flow before adding 50 µL of 3-(Acryloyloxy) propyltrimethoxysilane onto a glass block, and the cleaned side of the coverslip was placed on top for 1 h in a fume hood. The coverslips were individually rinsed with dd water and placed with the acrylsailnised side on top in a large petri dish, followed by two 5-minute washes with dd water on the shaker. Then, the coverslips were individually dried under N_2 flow. A different glass block is then sprayed with rainX and dried under nitrogen (N_2) flow before adding the corresponding amount of the gel mix to the coverslips used, as described in Table

2. The gels were then allowed to polymerise for 10 min, then lifted with tweezers and kept in dd water at 4°C to swell overnight.

2.3 PAAm hydrogel characterisation

2.3.1 Rheology

The stiffness of the gels was measured using an Anton Paar Modular Compact Rheometer (MCR 302e), and a strain sweep test was used at 1 Hz, 1% shear strain and normal force 0.1 N. For the characterisation, the gels were made using higher volumes of the PAAm gel mixture to be used for rheology. Both the 18 mm coverslips and the glass slides were cleaned and placed in rainX, and the amount used of the gel mix was 400 µL after allowing the gels to polymerise for 10 min both the coverslip and the glass slide were detached from the gels and kept in dd water at 4°C to swell overnight. A 15mm puncher was used to cut out the gel to fit the rheometer rod and measure the stiffness of the hydrogels.

2.3.2 Nanoindenter

The stiffness of 50mm gels was measured using an Optics11Life Chiaro Nanoindenter, with a prop tip radius of 3.5 µm from Optics11Life (serial number: P220730M). The gels were made as previously described, with two sets of three different stiffnesses made with different volumes of 50 and 100 µL. After allowing the gels to swell, the gels are glued to a flat bottom petri dish and then filled with water. A 5X5 matrix scan was performed on the gels to assess the uniformity of stiffness and to determine whether the gels made with two different volumes had similar stiffness.

2.4 Surface Coating Protein

The lights must be turned off for this part of the process as sulfo-SANPAH is light-sensitive. The gels were rinsed with dd water twice, then all the dd water was aspirated and 200 µL of sulfo-SANPAH (200 µm/mL in 50 mM HEPES pH 8.5) for 12 mm, 1mL for 30mm and 2mL for 50mm gel, the gels are immediately placed under a UV light source at a distance of 3 cm for 10 min, followed by three rinses with dd water to remove excess sulfo-SANPAH. For the incubation of the ECM proteins, 300 µL of collagen (40 µg in 50 mM HEPES pH 8.5) to the 12mm, 1 mL was used for

30mm gels and 2 mL for the 50 mm gels. The gels were incubated at room temperature for 1 h, followed by three rinses with dd water, and the gels were then stored at 4°C.

2.5 Nuclear and Cytoplasmic Extraction

The following kit, NE-PER Nuclear and cytoplasmic extraction reagents (ThermoFisher Scientific, Cat: 78833), was used in this experiment. First, the cells were harvested using trypsin-EDTA solution (Gibco, cat: 2636962) and then centrifuged at 1200 rpm for 3 min, followed by a wash with PBS to suspend the cell pellet. The cells are then transferred into prelabelled Eppendorf and centrifuged at 500 g for 3 min. Then, the cells were washed with PBS and centrifuged at 500 g for 5 min. The supernatant layer was removed, and the cell pellet was left to dry before ice-cold CER-I to add to the cell pellet using manufacture instructions for the size of packed cell volume. The following ratio of the reagents was used (CER-I:CER-II:NER, Reagents at 200:11:100 µL, respectively), then the appropriate amount of CER-I according to the manufacturer instructions was added, followed by vigorously vortexed at the highest setting for 15 seconds and 10 min incubation at on ice. Then, the appropriate amount of CER-II was added, followed by vigorous vertexing at the highest setting for 5 seconds and 1 min incubation on ice. After the incubation, the cells were vigorously vortexed at the highest setting for 5 seconds before being centrifuged for 5 min at 16000g. The supernatant layer containing cytoplasmic extracts was immediately moved to precooled Eppendorf and placed on ice. To extract the nuclear fraction, the insoluble pellet was suspended in an appropriate amount of NER according to the manufacturer's instructions and vigorously vortexed at the highest setting for 15 seconds, placed on ice, and vigorously at the highest setting for 15 seconds every 10 min four, repeated four times. Finally, the Eppendorf was centrifuged for 10 min at 16000 g, and the supernatant containing nuclear extract was immediately moved to precooled Eppendorf, placed on ice and stored at -80°C.

2.6 Protein Quantification

2.6.1 BCA Assay

The first kit was the BCA assay kit (ThermoFisher Scientific, Cat: 23227), which was used to quantify the protein for western blots. Firstly, six-point standards of 1:1 RIPA lysis and extraction buffer (ThermoFisher, Cat: 89901) and bovine serum albumin (BSA) from the albumin standard provided in the kit were made, and 20 µL of protein lysis and 80 µL of RIPA into prelabelled Eppendorf for each sample. This was followed by preparing the working concentration of BCA by using 50:1 of reagents (A: B), respectively. Then 200 µL of the reagent's mixture was added into a flat bottom 96 well plate, making three replicates for the standards and the samples. After the well plate was loaded with the mixture, 25 µL of the samples and standards were added into three different wells, making three replicates for each of the samples and the standards. The plate was then covered with aluminium foil and placed on a shaker for 5min followed by 30 min incubation at 37 C°. Then, the plate is placed in a spectrophotometer and measured using the following protocol: 20 seconds continuous shake, then read at 570 nm using the TeromFIsher Scientific MULTISKAN FC.

2.6.2 Micro BCA Assay

The Micro BCA protein assay kit (TehrmoFisher, Cat: 23235) was used to measure the amount of collagen adsorbed on the surface of the PAAm gels. First, standards of collagen with the following concentrations: 1600,800,400,200, and 0 µg/mL were used in the experiment. These were used as standards, and this was followed by preparing the working concentration of the Micro BCA reagents (25:24:1, Reagent Micro BCA Reagent A: Micro BCA Reagent B: Micro BCA Reagent C). After the 1 h incubation at room temperature of collagen, the remaining collagen was collected into a prelabelled Eppendorf for the measurements. Then 150 µL of the reagent's mixture was added into a flat bottom 96 well plate, making three replicates for the standards and the samples. After the well plate was loaded with the mixture, 150 µL of the samples and standards were added into three different wells, making three replicates for each of the samples and the standards. The plate is then covered with Aluminium foil and placed on a shaker for 30 seconds, followed by 2 h incubation at 37 C° Then the plate is placed in a

spectrophotometer and measured using the following protocol: 20 seconds continuous shake, then read at 570 nm using the TehrmoFisher Scientific MULTISKAN FC.

2.7 Cell Culture

PAT1S primary GBM cells extracted from a Taiwanese patient were cultured using Dulbecco's modified Eagle's medium (DMEM, high glucose, L-Glutamine, Sodium Pyruvate, Gibco, cat:2676166) with 10% foetal bovine serum (FBS, TehrmoFisher cat: 10 500-064), 1% Penicillin-streptomycin (Sigma-Aldrich, cat: P0781) and 0.004% of Amphotericin B(Gibco, Cat: 2556000). The media was changed every 2 to 3 days; when the cells were at 70% confluency, cells were washed using Dulbecco's phosphate-buffered saline (DPBS) and TryLE Express (Gibco, cat: 2636962) for 3 min in the incubator at 37°C to passage the cells. ALL cells used in this project were lower than passage 19.

2.8 Immunofluorescence

Cells were seeded on 12mm gel with different stiffnesses, at 2000 cm^{-2} for 7 days; media was changed on days 3 and 5. On day 7, the media was aspirated, and the cells were fixed using 4% formaldehyde at room temperature for 15min. The gels were washed with DPBS three times for 5 min, and 0.05% of Triton X-100 was used to permeabilise them for 10 min. The cells were blocked for 1h at room temperature and then incubated with the primary antibody diluted in 2% BSA overnight at 4°C and in a humidified chamber. The flowing day cells were washed three times using PBS. The secondary antibodies (Alexa Fluor 568-conjugated goat anti-rabbit (TehrmoFisher, Cat: A-11011, 1:500) or Alexa Fluor 647-conjugated donkey anti-mouse (TehrmoFisher, Cat: A-31571, 1:500) were diluted in 2% BSA and incubated in the dark for 1h at room temperature. Finally, the samples were washed three times with PBS and covered with aluminium foil; mounting media (TehrmoFisher, Cat: P36962) was used to mount the gels up on the glass slide where the gels were placed on top, and a drop of the mounting media was placed on top, a rectangular coverslip was placed on top of the mounting media and allowed to dry overnight in the dark before being sealed with nail polish. The samples were imaged using a confocal microscope (Zeiss LSM 880 confocal microscope with Airyscan) at 40X.

2.9 Gene Expression Profiling

PAT1S cells were seeded at 4000 cm^{-2} on gels with different stiffnesses to assess relative change in EMT and CSC markers. 30 mm gels were coated with 40 µg of collagen of varying stiffness were placed in 6-well non-tissue-culture-treated plats, washed three times with DPBS and UV-sterilized for 45 min with the plate cover removed. Cells were seeded in complete media and allowed to grow for 7 days; the media was changed on days 3 and 6.

2.9.1 RNA Extraction

The extraction of tRNA was done using Trizol (thermoFIsher, cat: A33250), where 1ml was used for each well after the gels had been moved to a new 6-well plate. The Trizol was moved into prelabelled Eppendorf, and 200 µL of chloroform was added to separate the aqueous and organic phases. The Eppendorf was vigorously shaken, kept at room temperature for 3min, and centrifuged at 12000 g for 15 min at 2 °C. The supernatant layer was moved to a pre-cooled Eppendorf, and 500 µL isopropanol was added to the precipitate, followed by vigorous shaking, inculcation on ice for 10 min and centrifuged at 12000 g for 15 min at 2 °C. Then, isopropanol was removed, and the pellet was washed three times using ice-cold 80% ethanol at 7500RPM for 5min. 20 µL of nuclease-free water (ThermoFisher, Cat: AM9938) was used to dissolve the tRNA pellet and quantified using Nanodrop2000. The purity of the tRNA was determined using the $OD_{260/230}$ and $OD_{260/280}$ (optical density).

2.9.2 Revers Transcription

1 µg or 3 µg of the RAN extracted was used for reverse transcription. Firstly, ezDNase was used to remove genomic DNA contamination following the manufacturer's instructions followed by the SuperScript IV reverse transcriptase system (ThermoFisher Scientific, Cat: 12595025). The quantification of the expression genes of interest was performed by PCR using 2x QuantiNova SYPER green PCR master Mix (QuantiNova PCR Kits, Cat: 208252), and ROX(6-carboxyl-X-Rhodamine) was used as passive reference dye. A reaction mixture of 10 µL was run on a 7500 Real-Time PCR system machine (Applied Biosystems) in Fast 96-Well plated (Applied Biosystems, Cat: 4346907).

2.9.3 Quantitative Real-Time PCR (qRT-PCR)

First, a mixture was made containing 3 µL the nuclease-free waster (NFW), 7 µL cDNA,7 µL of primer and 20 µL QuantiNova SYPER green PCR master Mix. Then, A reaction was run on 10 µL of the mixture on a 7500 Real-Time PCR system machine (Applied Biosystems) in Fast 96-Well plate (Applied Biosystems, Cat: 4346907) for three replicates of the gene of interest and the housekeeping gene.

Table 3. PCR primers sequences list.

Gene	Forward	Reverse
GAPDH	AGC CTC AAG ATC ATC AGC AAT	GTC ATG AGT CCT TCC ACG ATA C
RhoA	GAG AGA TGG TGT CTT GCT ATG T	GGC AGC CAT TGA TCT TTA ATC C
ROCK1	GGA TTG TTT GCT GGA TGG ATT G	TCG TAC CAT GCC TTC CTT ATT C
ROCK2	GAT TGG TGG TCT GTA GGT GTT	GGA GCT GCC GTT TCT CTT AT
E-Cadherin	CGA CCC AAC CCA AGA ATC TAT C	AGG TGG TCA CTT GGT CTT TAT TC
N-Cadherin	GGG ATC AAA GCC TGG AAC ATA	GAC ACG ATT CTG TAC CTC AAC A
Vimentin	AGG CAA AGC AGG AGT CCA CTG A	ATC TGG CGT TCC AGG GAC TCA
Vinculin	TGA GCA AGC ACA GCG GTG GAT T	TCG GTC ACA CTT GGC GAG AAG A
TJP1(ZO-1)	GTC CAG AAT CTC GGA AAA GTG CC	CTT TCA GCG CAC CAT ACC AAC C
FN	ACA ACA CCG AGG TGA CTG AGA C	GGA CAC AAC GAT GCT TCC TGA G
TGF-β	CGT GGA GCT GTA CCA GAA ATA C	CAC AAC TCC GGT GAC ATC AA
IL-6	AGA CAG CCA CTC ACC TCT TCA G	TTCT GCC AGT GCC TCT TTG CTG
SNAI1(Snail)	ACT ATG CCG CGC TCT TTC	GCT GGA AGG TAA ACT CTG GAT TA
SNAI2(Slug)	ATC TGC GGC AAG GCG TTT TCC A	GAG CCC TCA GAT TTG ACC TGT C
Twist	GCC AGG TAC ATC GAC TTC CTC T	TCC ATC CTC CAG ACC GAG AAG G
ZEB1	GGC ATA CAC CTA CTC AAC TAC GG	TGG GCG GTG TAG AAT CAG AGT C
ZEB2	CAC ATA TGG CCT ACA CCT ACC	CAA GCA ATT CTC CCT GAA ATC C
NESTIN	GGC AGC GTT GGA ACA GAG GT	CAT CTT GAG GTG CGC CAG CT
CDC42	GCA CTT ACA CAG AAA GGC CTA AA	GGG CTCT GGA GAG ATG TTC ATA
CXCR4	GGG ATC AGT ATA TAC ACT TCA GAT AAC TAC	GAT GGT GGG CAG GAA GAT TT
Sox-2	CCA TCC ACA CTC ACG CAA AA	TAT ACA AGG TCC ATT CCC CCG

Oct-4	TCC CAT GCA TTC AAA CTG AGG	CCA AAA ACC CTG GCA CAA ACT
ABCG2	TAT AGC TCA GAT CAT TGT CAC AGT C	GTT GGT CGT CAG GAA GAA GAG
ALDH1A1	CCC TCA GAT TGA CAA GGA ACA	GGC TGG ACA AAG TAG CCT TTA
ITGβ1	ATG AAT GAA ATG AGG AGG ATT ACT TCG	AAA ACA CCA GCA GCC GTG TAA C
ITGβ2	TAG GAG CAC TTG GTG AAG AC	AGA CTG ATG TCC TGA CTT GC
ITGβ3	CTG CTG TAG ACA TTT GCT ATG A	GCC AAG AGG TAG AAG GTA AAT A
ITGβ4	ATT CCG GGT GGA TGG AGA CA	CTG CTG TAC TCG CTT TGC AG
ITGβ5	CTG TGG ACT GAT GTT TCC TT	GTA TGC TGG TTT TAC AGA CTC C
ITGβ6	ATT TCT CAA AGG ATG GTT CTG	AAG TAG TTC TAG CAA TCT GTG GA
ITGβ7	AGC AGC AAC AAC TCA ACT GG	TTA CAG ACC CAC CCT TCC TCT
ITGβ8	GTA CAC TCG AAC GAA GAC TGA CAA	CAC AAT GCT AAA CTC TCT CAC AGC
ITGα1	CCT GAG AAG AGG AGA GAT GGT A	GCT GTC ACT TGT TGC ACT TAA A
ITGα2	TAT ACA GGA GCC CTC TGA TGT	GAC CTT GGC AGT CTC AGA ATA G
ITGα5	ACT AGG AAA TCC ATT CAC AGT TC	GCA TAG TTA GTG TTC TTT GTT GG
ITGαv	GGA GCA CAT TTA GTT GAG GTA T	ACT GTT GCT AGG TGG TAA AAC T

2.10 Protein Analysis Using Western Blot

Cells were seeded at 4000 cells cm^{-2} for 7 days on gels with the three different stiffnesses, and the media was changed on days 3 and 6. On day 7, the gels were washed using ice-cold DPBS and moved to a new 6-well plate. 50 µL of a mixture was made containing RIPA lysis and extraction buffer (ThermoFisher, Cat: 89901) containing protease and phosphatase inhibitors (ThermoFisher Scientific, Cat: 78442) at 1× final concentration and EDTA solution (ThermoFisher, cat:1861275) at 1× final concentration. Then, the lysis was scraped and moved into a pre-cooled Eppendorf, followed by vortexing for 1 min and incubated on ice for 30min. Finally, the proteins were centrifuged at 13000 RPM for 30min at 2°C to be extracted, the supernatant was moved into a pre-cooled new Eppendorf, and the cell pellet was discarded. BCA assay kit (ThermoFisher Scientific, Cat: 23227) was used to quantify the protein, and equal amounts of proteins were added to the mixture of Bolt LDS (lithium dodecyl sulphate) sample buffer (ThermoFisher, cat::

B0007, final concentration 2×) containing Bolt sample reducing agent (ThermoFisher Scientific, Cat: B0009) at a final concentration of 1x to a fixed final volume of 50 µL, denatured at 70 °C for 10 min followed by 5min at 90°C. The mixture of protein and sample buffer were loaded onto 4-12% Bolt Bis-Tris gels (ThermoFisher Scientific, Cat: NW04122BOX) and sodium dodecyl sulfate–polyacrylamide gel electrophoresis (SDS-PAGE) was performed by running the gel at 125V for 70 min in MOPS NuPage running Buffer (ThermoFisher Scientific, Cat: NP0001).

The proteins were transferred using Bolt transfer buffer containing 20% methanol (ThermoFisher Scientific, Cat: BT00061) at 20 V, 160 mA for 70 min in a cooled environment onto PVDF (Polyvinylidene difluoride) membrane (Merck, Cat: IEVH85R). After the transfer to remove methanol, the membrane was washed three times with dd water and then blocked using ether 3% bovine serum albumin (BSA) or in 5% non-fat dry milk (NFDM, Santa Cruz, Cat: sc-2324) for 1 h at room temperature then incubated the primary antibody of interest overnight at 4°C on a shaker. The next day, the membrane was washed three times for 5 min using Tris-buffered saline containing 0.1% Tween-20 (TBST) and then incubated for 1 h at room temperature on a shaker with a secondary antibody depending on the species of the primary antibody. Protein bands were visualised using a chemiluminescent substrate (ThermoFisher Scientific, Cat: 34580). The protein band quantification was done using densitometry in ImageJ (National Institute of Health, USA).

Table 4. demonstrates the list of antibodies used for Western Blot.

Antibody	Catalogue number	Dilution
GAPDH	60004-1-Ig	1:1000
ß-actin	A5441	1:1000
ROCK1	sc-17794	1:100
CD133	66666-1-ig	1:1000
ABCG2	27286-1-ap	1:1000
ALDH1A1	66031-1-ap	1:1000
VIMENTIN	V6630	1:1000
POU5F1(OCT-4)	11263-1-ap	1:1000
YAP	4912s	1:1000
TGF-ß	2189-1-ap	1:1000

EGFR	orb670862	1:1000
SOX-2	66411-2-ig	1:1000
pMLC2	3671s	1:1000
VINCULIN	20874-1-ap	1:1000
NESTIN	19483-1-ap	1:1000
SNAI1(SNAIL)	13099-1-ap	1:1000

2.11 Statistical analysis

GraphPad Prism 8 software was used for data analysis. First, the data normality was checked to determine the type of post-hoc test for analysis. An unpaired t-test was used for parametric data, and the Mann-Whitney test was used for non-parametric data. For qPCR data and the Western blot experiment, the Kruskal-Wallis test, followed by Dunn's multiple comparisons test, was performed for the non-parametric data to evaluate the differences between the three stiffnesses (n=3 per stiffness).

All data was presented as mean values; error bars represent standard deviation, and n represents the number of replicates, shown in the figure title. $P_{value} < 0.05$ was considered statistically significant. The statistical significance levels are $P<0.05$, $P<0.01$, $P<0.001$ and $P<0.0001$ indicated by *, **,*** and ****, respectively.

3 Results

In this chapter, all the experiments were performed on three different stiffnesses to assess the response of the Rock signalling pathway to the stiffness changes. First, the gel stiffnesses were characterised using rheology and nanoindentation to identify the stiffnesses presented as Young's modulus (E) and ensure that the gels had reproducible stiffnesses. The gel protein coating characterisation followed this to investigate whether sulfo-SANPAH influenced cell adhesion and what protein to use as the gel surface coating. After identifying that collagen, a vital extracellular matrix component, was the most compatible with cells used in this project to facilitate attachment on all stiffnesses, the optimal concentration needed was determined using a morphological comparison of different amounts of collage on the three stiffnesses. The amount of collagen adsorbed was measured to examine for any differences between the stiffnesses and assess if the cells were responding to the stiffness or the ligand density.

After optimising the conditions for cell culture, quantitative real-time PCR was performed. This step was instrumental in investigating whether the stiffnesses had different influences on the gene expression of mechanotransduction, EMT, EMT transcription factors, and CSC markers. The results of this step provided a deeper understanding of the impact of stiffness on these genes. Then, protein levels corresponding to some of the previously mentioned genes were examined to assess the cellular response to stiffness comprehensively.

3.1 Rheology

To mimic the tumour microenvironment, we aimed to produce gels in a wide range of stiffnesses to allow for diverse cellular responses. The cell's response might not significantly change if the stiffness is not well-spaced. The stiffness results of gels are as follows: Pa(soft), Pa(medium) and Pa(rigid). Another goal of this experiment was to assess the reproducibility of these gels and how the stiffness would change in replicates of the same gels and across the gel surface. The results confirm that it was possible to fabricate the PAAm hydrogels of the desired stiffness with consistency, where the soft PAAm gels had a stiffness of

305.9±16.9Pa, medium being 10.5±0.4kPa and rigid being 34.9±5kPa as shown in Figure2 B.

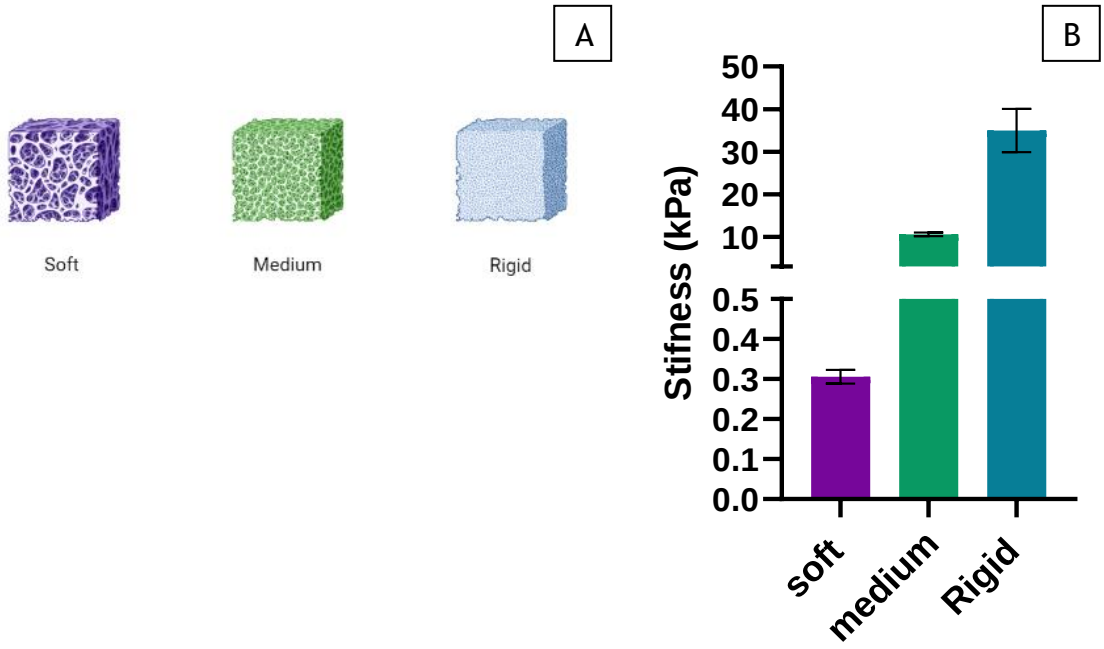

Figure 2. Rheology measurements of PAAm gel stiffnesses using a strain sweep test at 1Hz, 1% shear strain, and 0.1 N normal force. (A) (B) One point of the storage modules(G`) was taken for all the samples to obtain the stiffnesses. The averages ± standard deviation for the three stiffnesses (n=4) are shown.

3.2 Nanoindentation

The same gel stiffnesses previously mentioned in the rheology section were used, and two different volumes of the same stiffness were used to assess the stiffness and uniformity across the surface of the gel as it is much bigger compared to 12, 18, and 30mm used in other experiments. As shown in Figure 3, for the soft gels, the two volumes, 50µL and 100µL showed different stiffnesses, of 140.3 ±6.0Pa and 321.7±59.8 Pa, respectively. Although the same gel mixture was used for both gels, the 50µL gels were much softer compared to the 100µL. For the medium stiffness, the two volumes, 50µL and 100µL, a different stiffness trend was observed where the measurements were 24.5±5.8kPa and 8.01±0.4kPa, respectively. The same trend was observed for the rigid gels, where the two volumes (50µL and 100µL) resulted in stiffness of 44.15±3.4kPa and 39.19±2.6kPa, respectively.

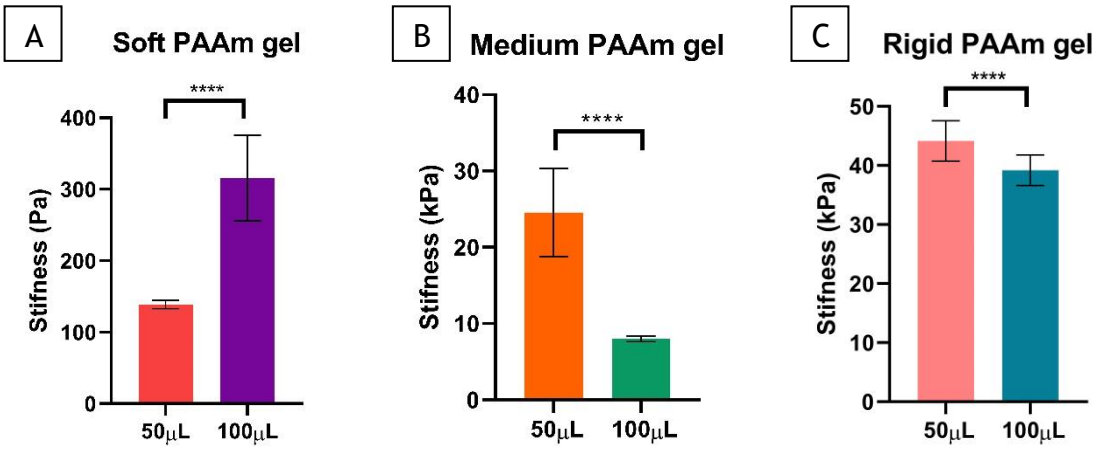

Figure 3. Nanoindentation measurements of PAAm gel stiffnesses using a 5X5 nanoindentation matrix scan. A) Soft PAAm hydrogels made of 50 and 100μL. B) Medium PAAm hydrogels made of 50 and 100μL. C) Rigid PAAm hydrogels made of 50 and 100μL. Data presented as mean ± SD and analysed t-test. ** indicates P<0.0001, (n=25).**

3.3 Protein Coating Characterisation

As the softer PAAm does not allow for cell attachment, it requires ECM protein for cells to attach and spread. The following treatments ECM protein treatments were chosen: control (no sulfo-SANPAH and ECM protein), sulfo-SANPAH, FN, Matrigel and Collagen type I. As shown in Figure 4, the control sample of soft hydrogel had a low number of cells attached but did not spread as a result of the stiffness. The same thing was observed in the FN and Matrigel samples. There was a minor increase in the number of the cells attached; however, they did not spread. This indicates that the concentrations used were low, and higher concentrations might show an improvement in the number of cells attached. The sulfo-SANPAH sample showed a response similar to Matrigel and FN. The reason behind that remains elusive. For collagen type I, a high number of cells were attached and spread. This illustrates that collagen type I facilitated cell attachment; nevertheless, as a result of the high concentration, cells spread more compared to the ones on FN and Matrigel. Figure 5 shows medium hydrogels; the control sample cells' attachment and spreading were similar to the control of soft hydrogel. The following treatment, sulfo-SANPAH, FN and Matrigel, showed the same response on medium compared to the soft samples, which the low concentration of the ECM proteins could explain. Figure 5 shows the cell morphology on rigid PAAM hydrogels; on the control sample, the cells attached and spread as a result of the high stiffness, and the same thing was observed on the sulfo-SANPAH sample. For

FN and Matrigel samples, the stiffness facilitates more cell attachment. However, the cell spreading was restricted as a result of low concentrations of the proteins. For collagen type I, the same response of soft and medium gels was observed on the rigid hydrogels, possibly due to the high concentration of collagen used.

Collagen type I was the best option as the cells attached and spread to all stiffnesses, but the optimal concentration of collagen has yet to be found, which led to the next experiment in which a variation of collagen concentrations was used to decide what collagen concentration to be used for the subsequent part of the project. The cell morphology dramatically changed due to the increased stiffness as the cell morphology was more rounded on the soft PAAm cells than the medium and rigid. The more cells spread, the more stress fibres are formed on the rigid hydrogels compared to soft ones, translating into more spreading (Acharekar et al., 2023; Grundy et al., 2016). In Figure 7, reducing the concentration of collagen type I shows the same trend among all stiffnesses, where cells attached to the gels coated with collagen and only a few cells were attached to the control gels. Still, the cell morphology is the same despite decreasing concentration, indicating that the response is due to the stiffness, not the amount of protein. The optimal concentrations were 20 and 40 µg/mL, as the number of cells attached was relatively the same for all stiffnesses.

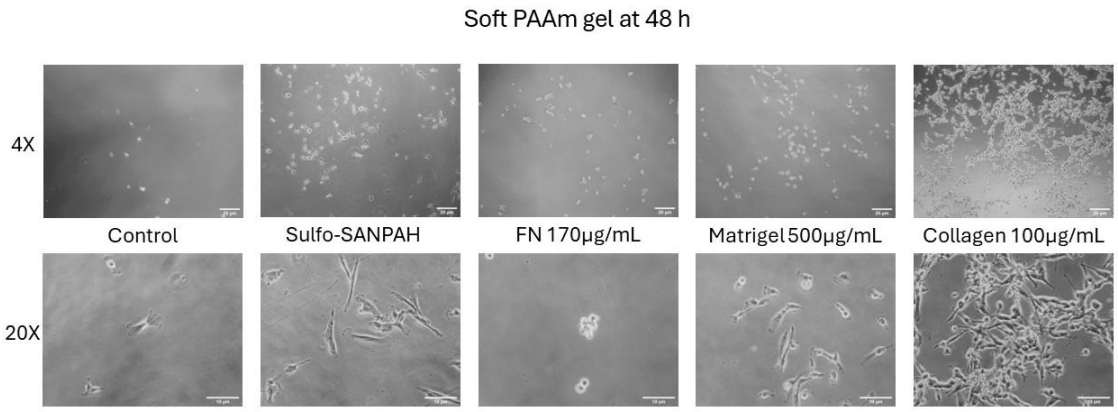

Figure 4. Optical microscopy images of soft PAAm gel at 48 h with different conditions control (no sulfo-SANPAH and ECM protein), sulfo-SANPAH, FN at 170 µg/mL, Matrigel 500 µg/mL and collagen at 100 µg/mL. They show collagen to have the best compatibility compared to other conditions (4X scale bar, 25 µm and 20X scale bar, 10µm).

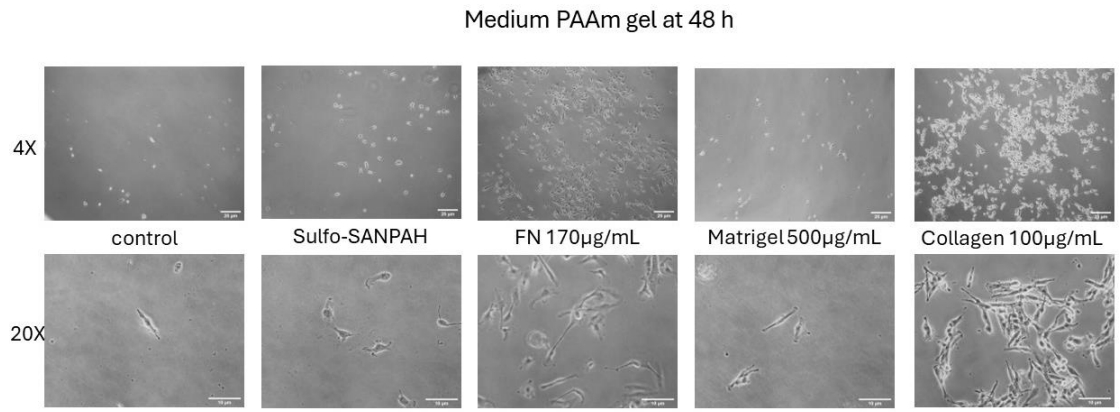

Figure 5. Optical microscopy images of medium PAAm gel at 48 h with different conditions control (no sulfo-SANPAH and ECM protein), sulfo-SANPAH, FN at 170 µg/mL, Matrigel 500 µg/mL, and collagen at 100 µg/mL. Collagen has the best compatibility compared to other conditions (4X scale bar, 25 µm and 20X scale bar, 10µm).

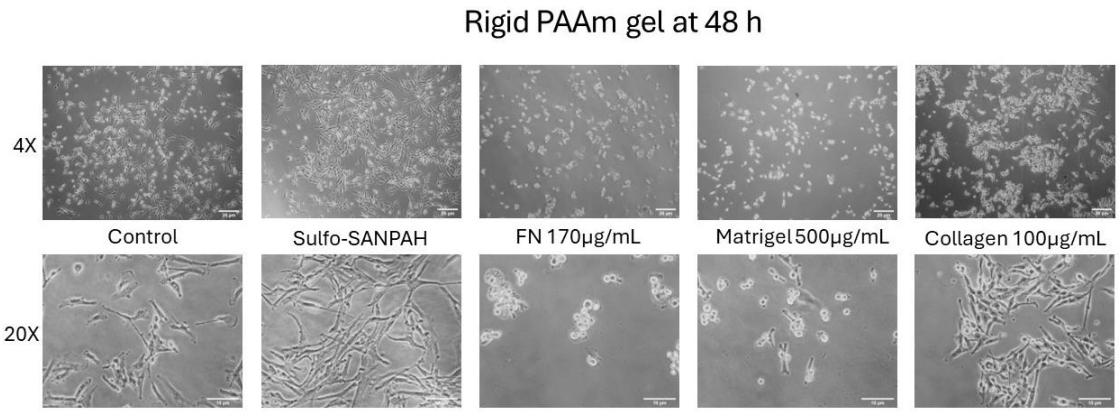

Figure 6. Optical microscopy images at 48 h of rigid PAAm gel with different conditions control (no sulfo-SANPAH and ECM protein), sulfo-SANPAH, FN at 170 µg/mL, Matrigel 500 µg/mL, and collagen at 100 µg/mL. Collagen has the best compatibility compared to the one control due to the PAAm gels' stiffness (4X scale bar, 25 µm and 20X scale bar, 10µm).

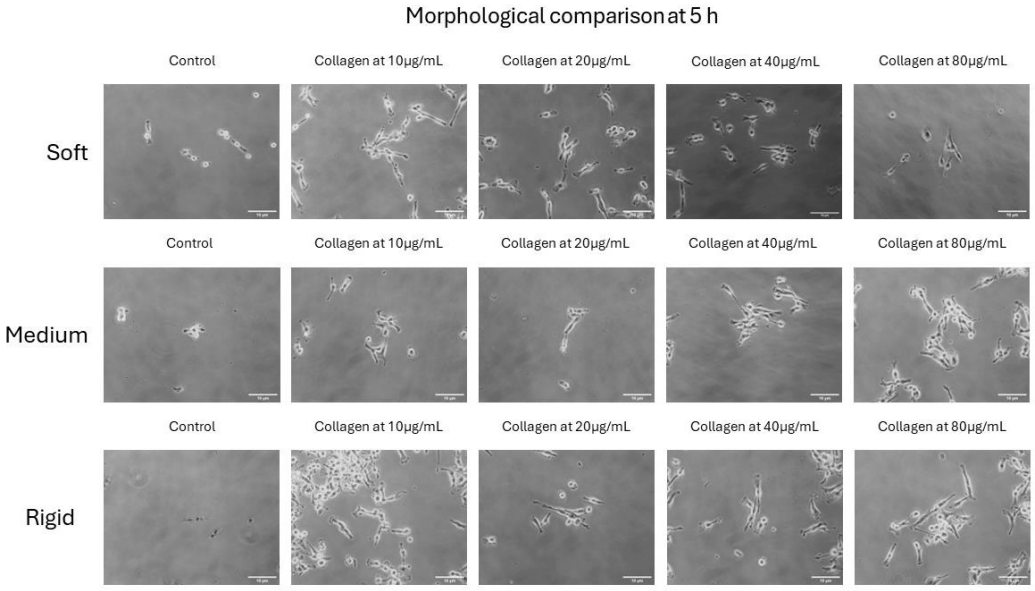

Figure 7. Optical microscopy images with 20X objective at 5 h of the three different stiffnesses with control (no sulfo-SANPAH and ECM protein) and collagen concentration of 10,20,40 and 80 µg/mL. As shown, the cell numbers on the three stiffness mainly were similar to the 20 and 40 µg/mL (20X scale bar, 10µm).

3.4 Collagen Quantification

The next question was whether the response was due to the ligand density or the stiffness, as it has been shown that high ligand density will allow the cell to form more focal adhesion and spread more even on soft substrates (Stanton et al., 2019). To answer that question, the amount of collagen adsorbed on the three stiffnesses was measured at two different concentrations, and no statistical significance was found between the amounts adsorbed on the stiffnesses at two different concentrations. This indicates that the cellular response was due to the stiffness, not the ligand density, as shown in Figure 8. Due to no significant differences found across the stiffnesses, 40 µg/mL was used for the following experiments.

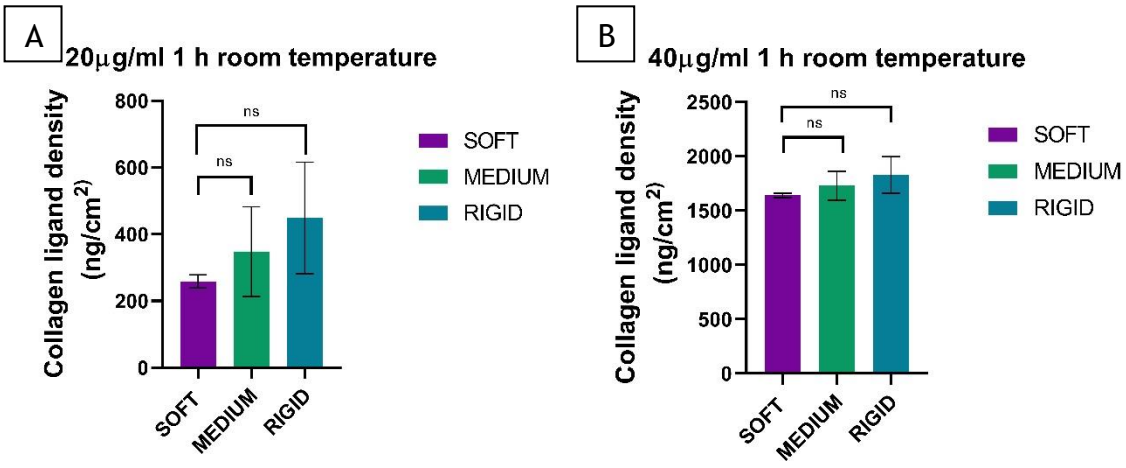

Figure 8. Quantification of the amount of collagen adsorbed to the gel surface. The data are presented as the mean ± standard deviation and were analysed with one-way ANOVA and Tukey post-hoc test. There were no statistically significant differences between the samples (ns). Results show the amount bound to the PAAm gel surface after 1 h coating at room temperature.

3.5 YAP Localisation

YAP localisation allowed the assessment of the cell's ability to sense the stiffness of the gels; this experiment was done to assess if the YAP translocation is different amongst the three stiffnesses. As shown in Figure 9 A, YAP was mainly localised in the cytoplasm on the soft gels. As the stiffness increases, the amount of YAP localised in the nucleus increases due to the stiffness, indicating that the cells can sense and respond to the stiffness, not to the ligand density, where it was the same on all stiffnesses (Stanton et al., 2019). This is also highlighted in the nuclear and cytoplasmic fractions (Figure 9 B), where a stiffness-dependent response was found. The ratio of nuclear to cytoplasmic YAP was higher on medium for the three replicates and rigid for the three replicates compared to soft gel (Figure 9A); as the stiffness increases, more YAP relocates to the nuclease, resulting in increased nuclear to cytoplasmic YAP ratio. Although the ratio of nuclear to cytoplasmic YAP was less on two of the replicates compared to the medium, it might be due to it being closer to the native stiffness of the tumour tissue, which is around 11.4 kPa (Bhargav et al., 2022). This was further illustrated using immunofluorescent imaging shown in Figure 10 A, where YAP was localised in the cytoplasm on the soft PAAm gel compared to medium and rigid PAAm gels shown in Figures 10 B and C, where the YAP is mainly localised in the nucleus, confirming that the cellular response is due to the PAAm gel stiffness, not the ligand density.

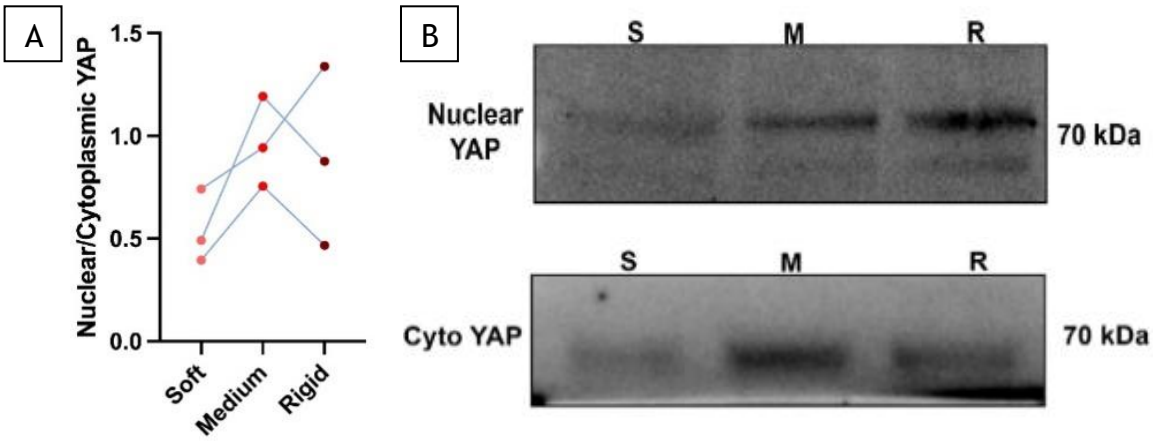

Figure 9. Immunoblots showing YAP nuclear and cytoplasmic fractions. (A) Quantification of nuclear YAP over the cytoplasmic YAP. (B). Immunoblots of the nuclear and cytoplasmic fraction of YAP. GAPDH was used as a loading control, and soft hydrogel was used as a reference for quantification(A,n=3, each line indicating an Individual replicate). YAP localisation shows stiffness-dependent responses where more is translocated to the nucleus as the stiffness increases.

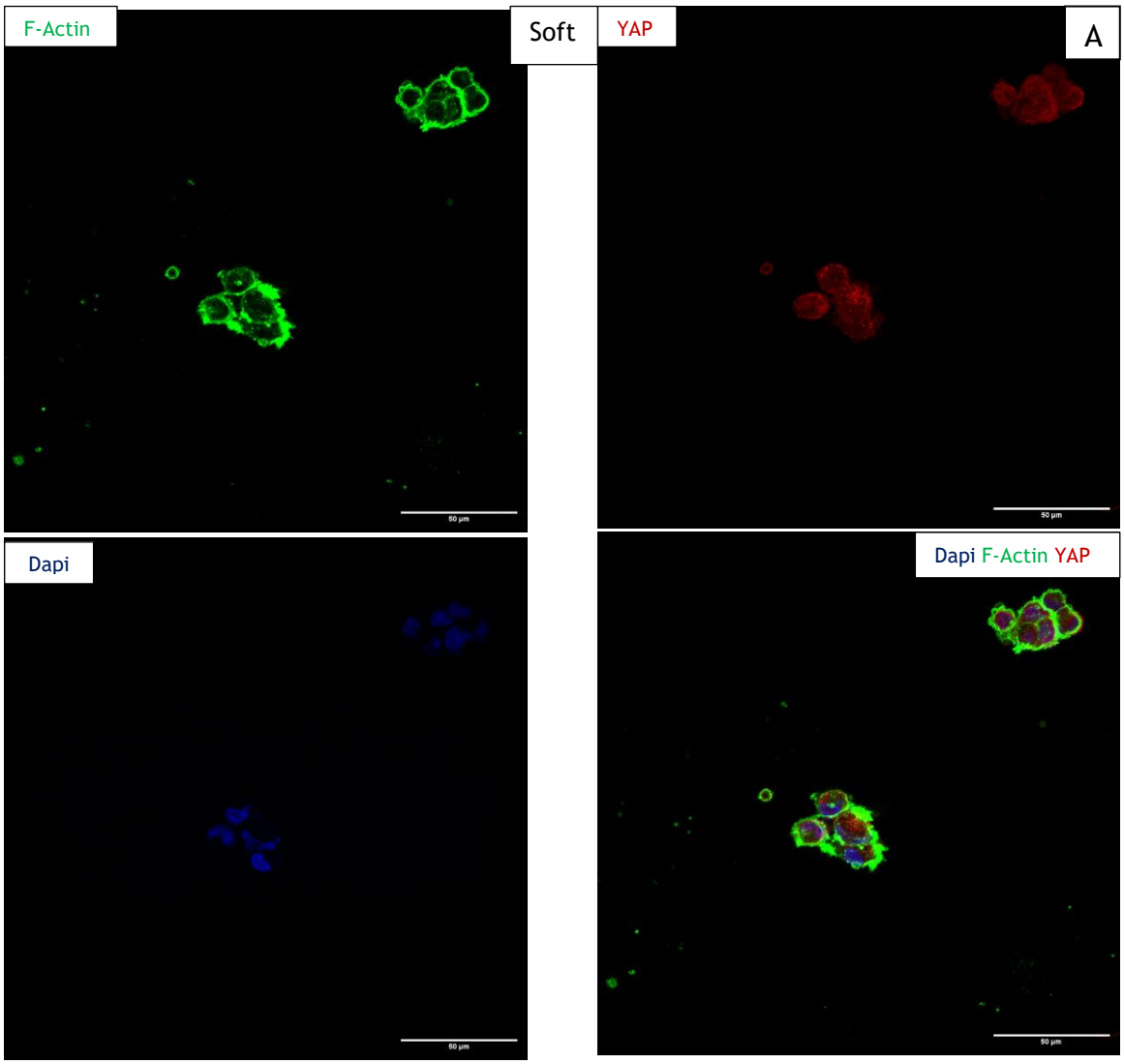

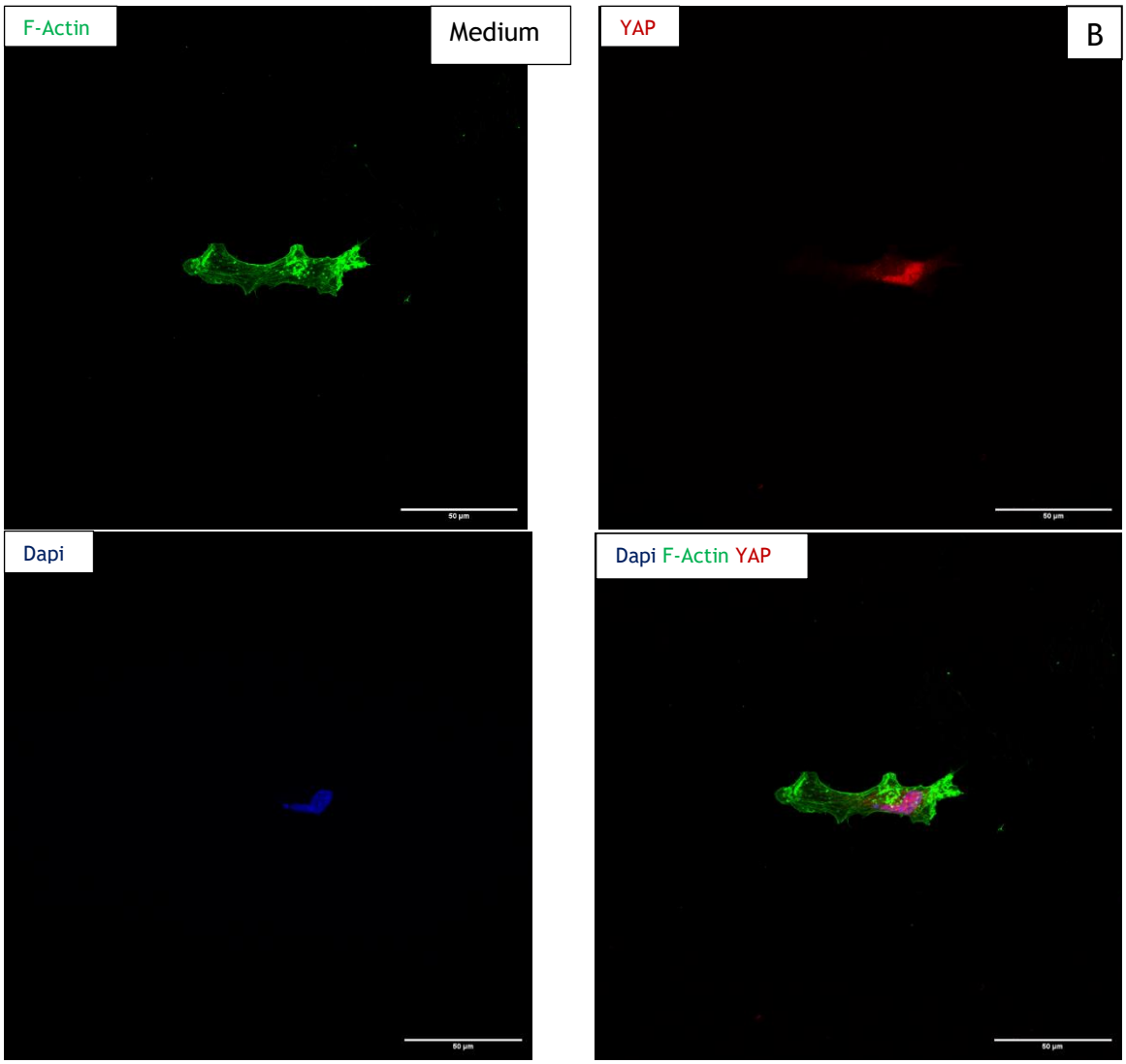
F-Actin
Medium
YAP
B
Dapi
Dapi F-Actin YAP

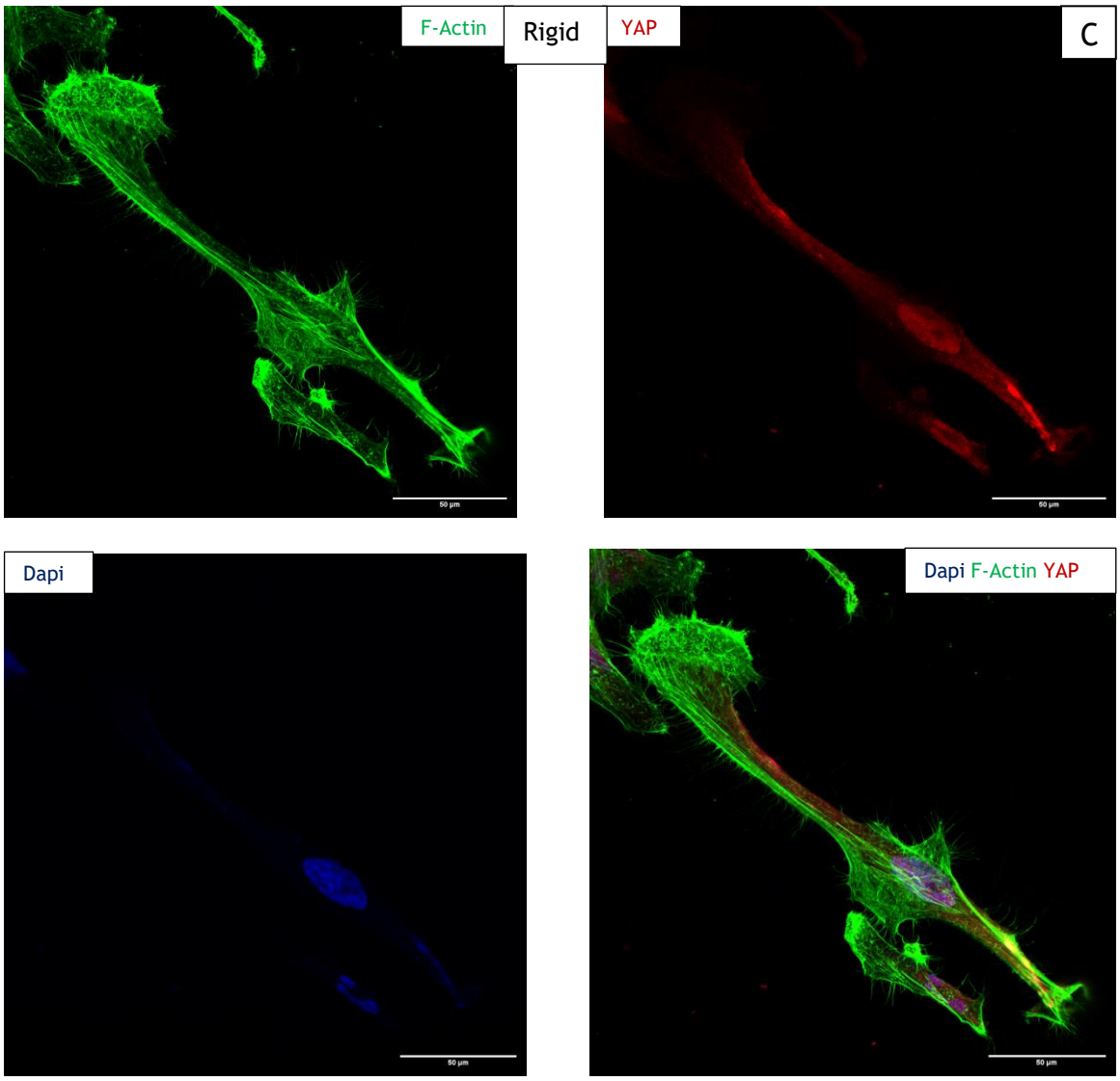

Figure 10. Immunostaining for YAP, F-actin and cell nucleus; showing YAP localisation in response to the three stiffnesses (scale bar 50 µm). (A) Immunofluorescent images of Soft PAAm hydrogel. (B) Immunofluorescent images of Medium PAAm hydrogel. (C) Immunofluorescent images of Rigid PAAm hydrogel.

3.6 Quantitative Real-time qPCR

Quantitative PCR was used to assess the changes in mechanotransduction genes, integrin genes, EMT markers, EMT transcription factor, and cancer stemness (CSC) markers. This method allowed for accurately measuring the genes' expression levels of these markers. Cells were cultured for 7 days on soft, medium, and rigid gels for the following experiments. The soft PAAm gel was used as a control, and the genes normalised against glyceraldehyde 3-phosphate dehydrogenase (GAPDH) as the housekeeping gene.

3.6.1 Mechanotransduction Genes

This part investigated the relevant mechanotransduction genes such as RhoA, ROCK1, and ROCK2 due to their role in sensing and responding to mechanical

stiffness. Figure 11 shows the gene expression of some that are part of the ROCK signalling pathway, which is very dynamic and can, directly and indirectly, regulate the cytoskeleton (Sin et al., 1998). No statistical significance differences were observed, even though the expression of RhoA, ROCK1 and ROCK2 was upregulated as the stiffness increased. The medium and rigid hydrogels showed an increase in two of the three replicates compared to soft ones. The highest response was observed on the medium hydrogels for RhoA (-1.50±0.3), ROCK1(-0.3±0.5) and ROCK2(-0.5±0.9), respectively. These could be a consequence of stiffness being similar to GBM stiffness. This could be explained by the matrix stiffness contributing to the regulation of the cell cytoskeleton and increasing the gene expression of these mechanotransduction genes. However, as a result of the limited number of replicates and missing the optimal time point for the gene expression, no statistically significant change was observed. Further investigation at the protein level could show a higher response to stiffness change as they are responsible for cellular behaviour.

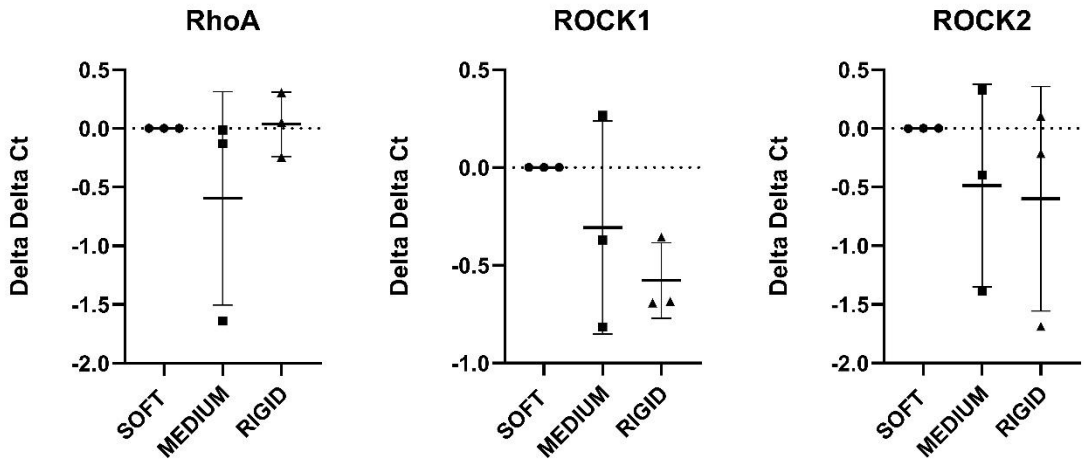

Figure 11. Real-time qPCR analysis of RhoA, ROCK1 and ROCK2 (mechanotransduction) gene transcription levels in response to the change in stiffness (n=3). No statistical significance was found. Shapiro-Wilk normality test, Kruskal-Wallis test, followed by Dunn's multiple comparisons test. The data is presented as delta delta ct ± standard deviation. The soft PAAm gel was used as a control, and the gene expression was normalised against glyceraldehyde 3-phosphate dehydrogenase (GAPDH), which was used as the housekeeping gene.

3.6.2 EMT Markers Genes

These markers can be categorised into two groups: mesenchymal markers and epithelial markers. For the cells to undergo EMT, they lose some of their epithelial

characteristics and gain some characteristics. Figure 12 shows the gene expression of EMT genes on the three stiffnesses; there was a decrease in the medium and rigid hydrogels in response to stiffness increase in the expression of two epithelial markers, TJP1(ZO-1) and Vinculin, although not statistically significant. The results showed a decrease in gene expression of TJP(ZO-1) on medium (0.3±0.5) and rigid (0.3±0.3), respectively. TJP1(ZO-1) is crucial for maintaining epithelial cell morphology, and the decrease in the gene expression can induce the EMT program (Georgiadis et al., 2010). The same trend was observed in the gene expression of Vinculin on medium (0.7±0.8) and rigid (0.4±0.5), respectively. However, E-CAD, another epithelial, showed an increase in gene expression in responses to stiffness increase where the gene expression increased on medium (-1.5±3.3) and rigid (0.5±0.3.3) hydrogels, respectively. Nevertheless, it was not statistically significant. This increased E-CAD expression could be explained by increased cancer stemness capabilities, as increased E-CAD expression was associated with enhanced cancer stemness properties (Lewis-Tuffin et al., 2010; Noronha et al., 2021). For mesenchymal markers, the following markers N-CAD, FN and TGF-ß showed a decrease in the gene expression in response to stiffness; however, it was not statistically significant. The gene expression of N-CAD was decreased in response to the stiffness increases on the medium (0.15±0.3) and rigid (0.1±0.1) hydrogels, respectively. The same was observed in the gene expression of FN; there was a decrease in the expression on medium (0.8±0.9) and rigid (0.6±0.2) hydrogels, respectively. TGF-ß showed the same response where the gene expression was decreased on the medium (0.2±0.19) and rigid (0.3±3), respectively. For VIMENTIN, a mesenchymal marker, there was a significant decrease in the expression on the medium PAAm hydrogels ($p < 0.05$) and rigid PAAm ($p < 0.01$) in response to stiffness increase. The gene expression was downregulated on the medium (0.3±0.16) and rigid (0.4±0.03) hydrogels, respectively. This could be an indication that the cells are unedging EMT as stiffness increases, prompting the loss of some epithelial characteristics (Fang & Kang, 2021; Kröger et al., 2019; Lu & Kang, 2019). However, the assessment of these markers at the protein level would provide a more relevant response as they conduct changes in the cells.

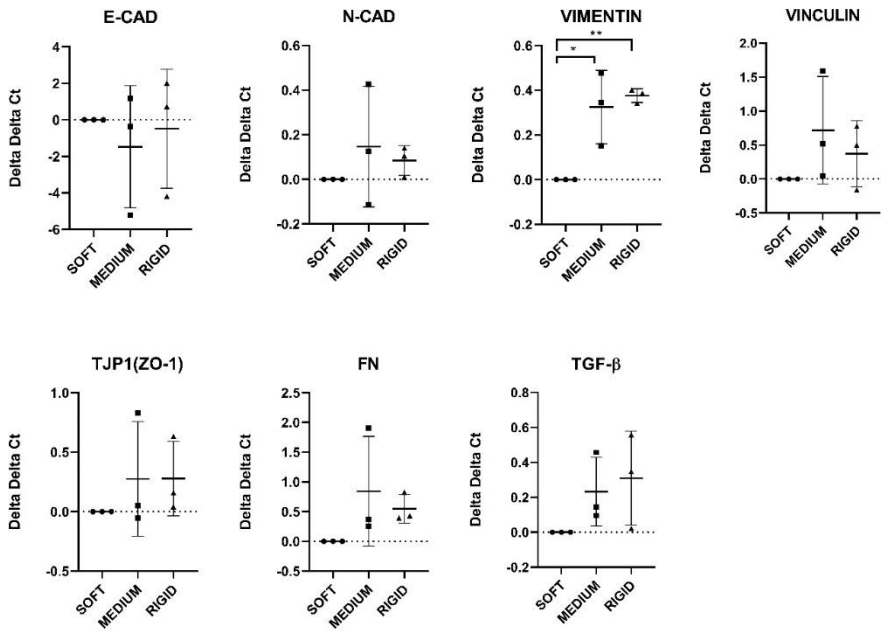

Figure 12. Real-time qPCR analysis of EMT markers genes transcription levels in response to the change in stiffness (n=3) Vimentin shows a statistically significant change due to stiffness, compared to the other markers, which also show a similar change but not statistically significant. Shapiro-Wilk normality test, Kruskal-Wallis test, followed by Dunn's multiple comparisons test. The data is presented as delta delta ct ± standard deviation. The soft PAAm gel was used as a control, and the gene expression was normalised against glyceraldehyde 3-phosphate dehydrogenase (GAPDH) as the housekeeping gene; * and ** indicate p<0.05 and 0.01, respectively.

3.6.3 EMT Transcription Factors

EMT transcription factors were investigated for their role in the promotion of mesenchymal markers and suppression of E-CAD (Ansieau et al., 2014). No statistical differences were observed in Figure 13; the following transcription factors, SNAI2(SLUG), SNAI1(SNAIL), and ZEB1, were downregulated in response to the increased stiffness. This is an unexpected trend where the EMT transcription factors gene expressions are upregulated in response to high stiffness(Matte et al., 2019). An increase in the gene expression of ZEB2 was observed in the medium (-0.25±0.31) hydrogels compared to soft ones; however, there was a decrease in the rigid (0.1±0.19) hydrogels compared to soft ones. For TWIST, the gene expression was upregulated on the medium (-0.5±1.1) and rigid (-0.6±0.9) hydrogels compared to the soft ones. This was consistent with the data shown in the previous section, which shows that gel stiffness could have promoted the cells to go through EMT. As mentioned previously, EMT is a reversible process with an intermediate stage, and the cell response might be in any stage of that process.

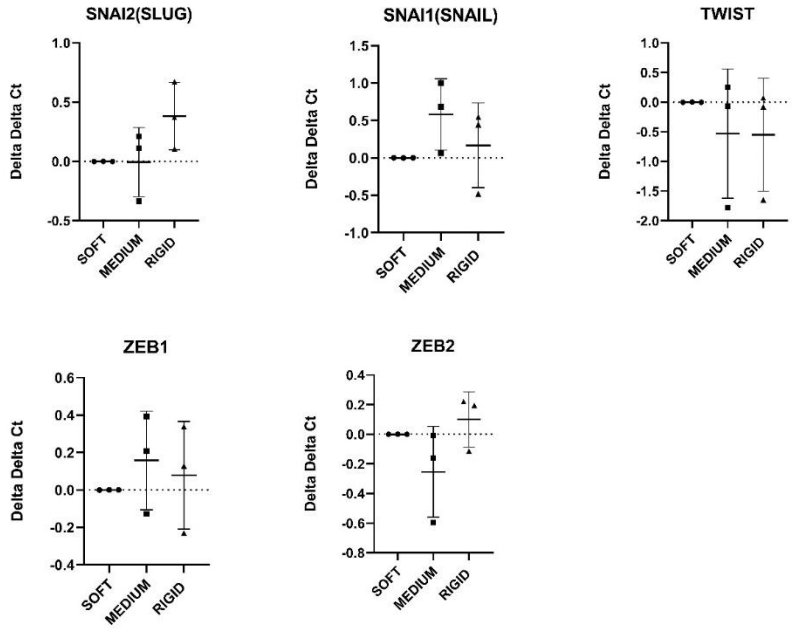

Figure 13. Real-time qPCR analysis of EMT transcription factors genes transcription levels in response to the change in stiffness (n=3) No statistical significance was found; Slug and Snail showed the highest response to the change in stiffness compared to the other transcription factors. Shapiro-Wilk normality test, Kruskal-Wallis test, followed by Dunn's multiple comparisons test. The data is presented as delta delta ct ± standard deviation. The soft PAAm gel was used as a control, and the gene expression was normalised against glyceraldehyde 3-phosphate dehydrogenase (GAPDH), which was used as the housekeeping gene.

3.6.4 Cancer Stem cells (CSC) Markers

These cancer stemness(CSC) markers were investigated to assess the influence of mechanical stiffness on the cancer stemness of GBM cells. No statistical differences were observed in the gene expression of the following CSC markers: NESTIN, CDC42 and SOX-2. However, their gene expression was upregulated due to the increase of the stiffness, as shown in Figure 14. There was a significant increase in the gene expression of ABCG2 ($P<0.05$) on the rigid (-0.5±0.16) hydrogels, and an increase was observed on the medium (-0.3±0.3) hydrogels. However, it was not statistically significant. A significant increase was observed in the expression of CXCR4 ($P<0.05$) on the rigid (-0.3±0.19) hydrogels compared to soft, and an increase was observed in the expression of medium (-0.3±0.2) compared to the soft hydrogels, although not significant. The gene expression of POU5F1(OCT-4) was increased on the medium (-0.2±0.19) hydrogels and significantly decreased on the rigid (0.3±0.13) compared to the medium ($P<0.05$). This could be explained by the fact that medium stiffness was similar to GBM stiffness, and the rigid was much higher than the physiological stiffness of GBM. There was a statistically significant decrease in the gene expression of ALDH1A1

(P<0.001) on the medium (1.1±0.12) and rigid (1.18±0.3) hydrogels compared to soft. This might be explained by a negative feedback loop to prevent the proteins from accumulating excessively (J. Kim et al., 2020).

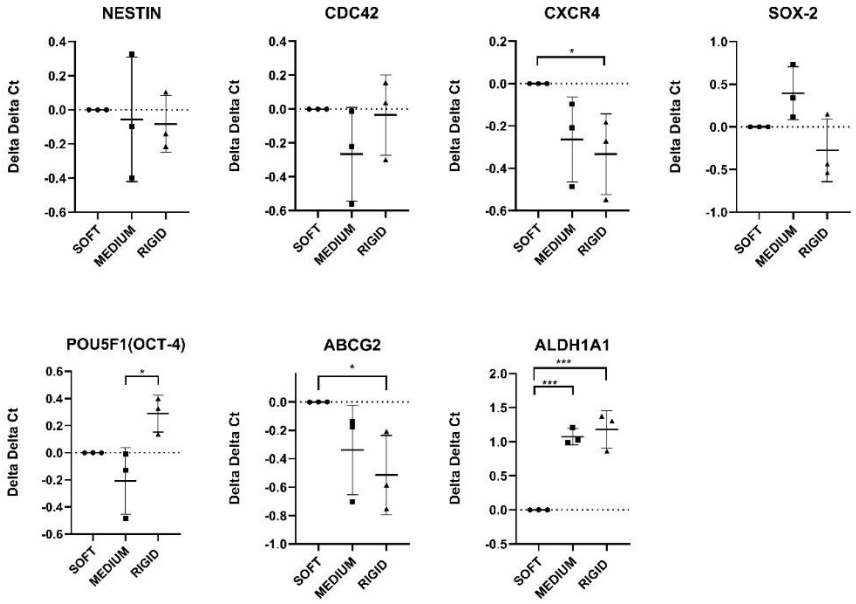

Figure 14. Real-time qPCR analysis of Cancer stem cells (CSC) markers genes transcription levels in response to the change in stiffness (n=3). CXCR4 and ABCG2 showed a statistically significant increase in gene expression compared to POU5F1, which showed a statistically significant decrease. Although NESTIN, a CSC marker specific to GBM, did not show a significant change. Shapiro-Wilk normality test, Kruskal-Wallis test, followed by Dunn's multiple comparisons test. The data is presented as delta delta ct ± standard deviation. The soft PAAm gel was used as a control, and the gene expression was normalised against glyceraldehyde 3-phosphate dehydrogenase (GAPDH) as the housekeeping gene; * and * indicate p< 0.05 and 0.001, respectively.**

3.6.5 Integrin Genes

These integrin genes were investigated due to their involvement in sensing mechanical stiffness and force transmission (Campbell & Humphries, 2011; J. H. C. Wang, 2006). No statistical significance was observed amongst the set of integrin genes, as shown in Figure 15; however, some trends were observed where the following genes, ITGß2, ITGß6, ITGß8 and ITGα2, showed little to no change in response to the increase in stiffness. More specifically, the gene expression of ITGß2 was consistent throughout the three stiffnesses, whereas ITGß8 and ITGα2 showed a slight decrease in gene expression on the rigid gels (0.1±0.9) and (0.1±0.1), respectively. The opposite was observed for the ITGß6, where there was a slight increase in gene expression for the rigid gels (-0.3±0.6). However, integrins are known to facilitate communication processes between cell-ECM and

cell-cell (Israeli-Rosenberg et al., 2014; Iwamoto & Calderwood, 2015). Nevertheless, the expression of integrin complexes is cell-specific and dependent on cell type and developmental stage, which might explain the low changes in this set of integrins.

The following integrins, ITGß3, ITGß4, ITGß5, and ITGα5, showed decreased gene expression as stiffness increased. This response was consistent for the medium and rigid gels, which showed similar gene levels, best illustrated by ITGß3 and ITGß4 genes shown in Figure 15. The gene expression of ITGß3 observed on medium and rigid were (1.4±.01) and (0.89±1.14), respectively. For ITGß4, the gene expression observed was downregulated on the medium (1.3±0.4) and rigid (1.2±0.17) hydrogels. Although ITGß5 and ITGα5 showed similar trends, however, the change in gene expression was lower compared to ITGß3 and ITGß4 genes. the gene expression of ITGß5 was downregulated on the medium (0.32±0.56) and rigid (0.3±0.5) hydrogels. The same was observed on the gene expression of ITGα5, as there was a similar decrease in the medium (0.4±0.13) and rigid (0.16±0.19) hydrogels.

Lastly, the following genes, ITGß1, ITGß7, ITGα1 and ITGαv, showed an increased gene expression in response to the stiffness increase. Although ITGα1 and ITGß1 showed a slight increase, the trend was consistent as gene expression increased on medium and rigid gels compared to the soft. The gene expression of ITGα1 showed an increase in the medium (-0.4±0.4) and rigid (-0.15±0.3) hydrogels, respectively. For ITGß1, an increase was observed in gene expressions on medium (-0.4±0.13) and rigid (-0.24±0.65), respectively. A higher response to the change in stiffness in gene expression of ITGß7 and ITGαv further demonstrated this. The gene expression ITGß7 showed an increase in medium (-1.2±0.8) and rigid (-1.0±0.4) hydrogels, respectively. A similar increase was observed in the gene expression of ITGαv on the medium (-0.6±0.8) and rigid (-0.9±0.4) hydrogels, respectively.

In conclusion, the data indicated that the increase in stiffness influences the gene expression of the integrins, although no statistical significance was observed. These findings suggest that the following integrins, ITGß1, ITGß3, ITGß4, ITGß5, ITGß7, ITGα1, ITGα5, and ITGαv, are promising and worth investigating further as

they are fundamental for sensing the microenvironment of the cells and transmitting the force between the actin cytoskeleton and ECM.

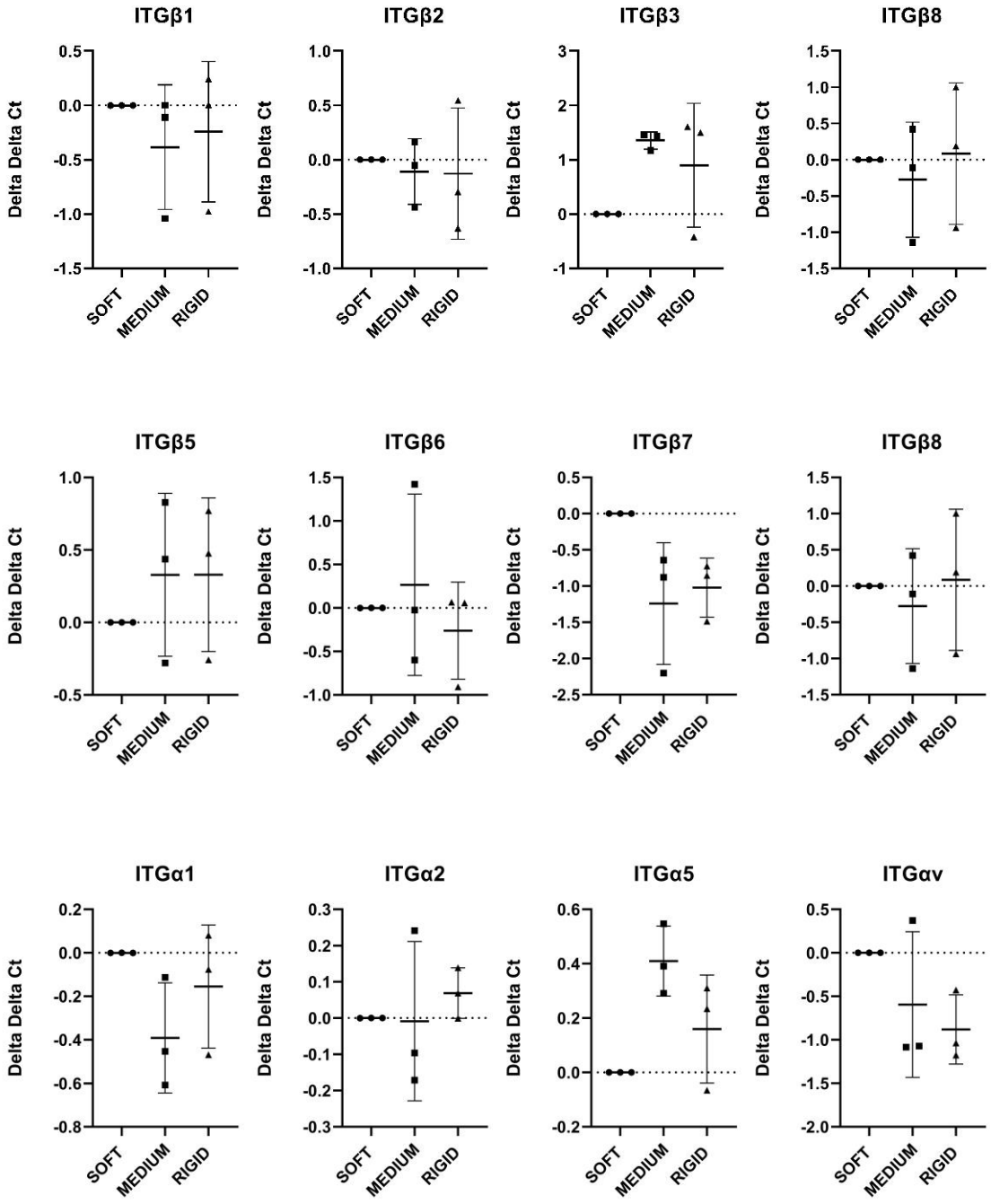

Figure 15. Real-time qPCR analysis of integrin genes transcription levels in response to the change in stiffness (n=3). No statistical significance was found. ITGβ1, ITGβ3, ITGβ4, ITGβ5, ITGβ7, ITGα1, ITGα5 and ITGαv showed the most change out of all the genes, although the change is not statistically significant. Shapiro-Wilk normality test, Kruskal-Wallis test, followed by Dunn's multiple comparisons test. The soft PAAm gel was used as a control, and the gene expression was normalised against glyceraldehyde 3-phosphate dehydrogenase (GAPDH), which was used as the housekeeping gene.

3.7 Immunoblots

These experiments were performed to assess the protein level and cell response to stiffness. First, some mechanotransduction proteins involved in the cellular response to stiffness were investigated, followed by EMT, EMT transcription factor, and CSC proteins, to assess their response to stiffness. The following experiments were performed after 7 days of cell culture to allow the cell to respond to stiffness expressed through protein expression. The immunoblots have been quantified and normalised against housekeeping proteins glyceraldehyde 3-phosphate dehydrogenase (GAPDH) or ß-Actin.

3.7.1 Mechanotransduction Proteins

The following mechanotransduction proteins, pMLC2 and VINCULIN, showed an increase in protein levels in response to the increased stiffness, illustrating that cells were able to sense the stiffness and respond as shown in Figures 16B, C, and D. Furthermore, there was a significant increase($P<0.05$) of the protein levels of ROCK1 on the medium (2.7 ± 1.02) hydrogels. The protein levels of ROCK1 were also increased on the rigid (1.6 ± 0.3) hydrogels. However, the change was not statistically significant, as shown in Figures 16 A and D. This might be due to the medium stiffness being close to the GBM stiffness.

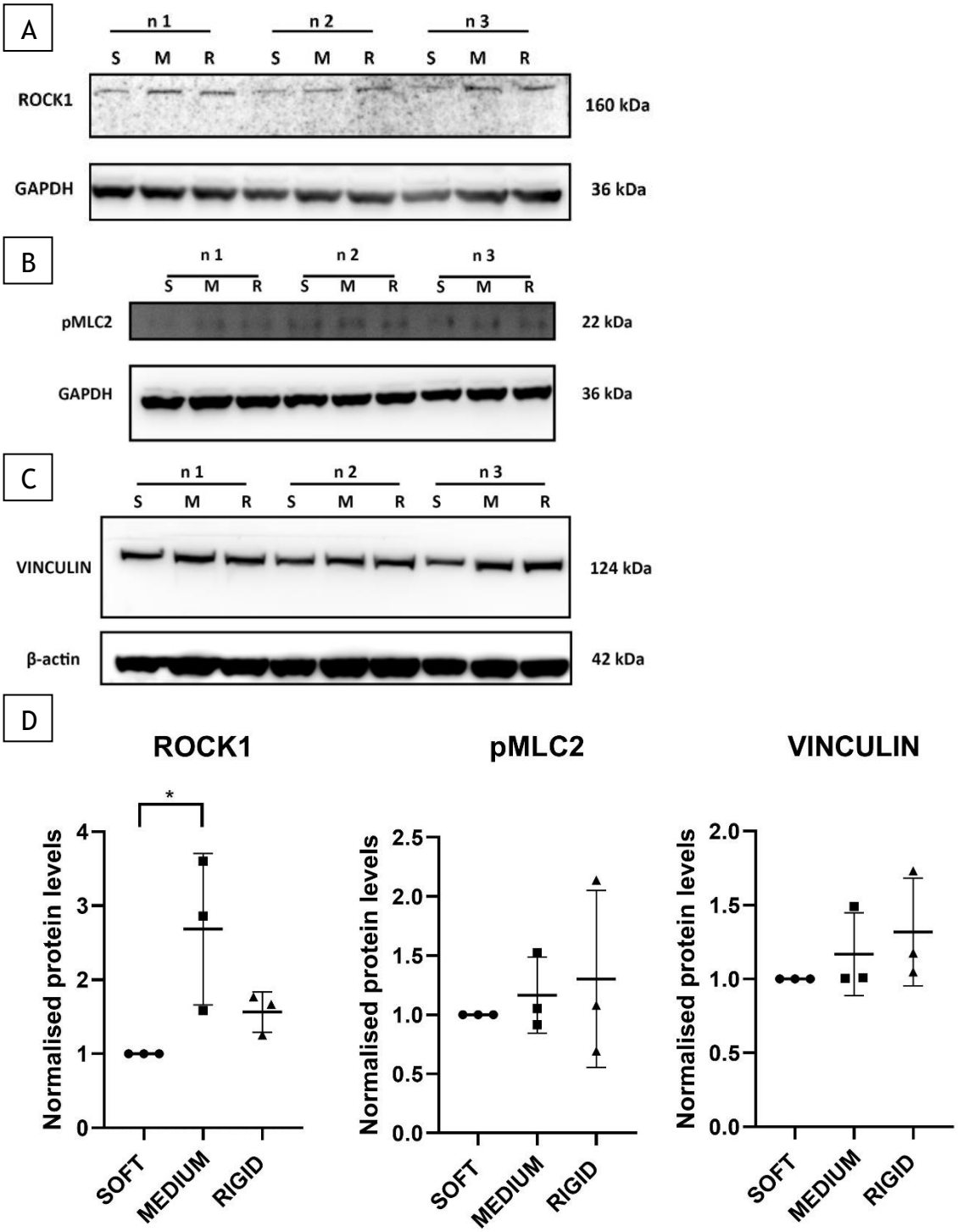

Figure 16. Immunoblot quantification of ROCK pathway protein levels in response to stiffness. (A-C) The immunoblots and the corresponding housekeeping proteins were used for quantification. (D) Quantification of ROCK1, pMLC2 and VINCULIN protein levels on the soft, medium and rigid hydrogels. (n=3). Shapiro-Wilk normality test, Kruskal-Wallis test, followed by Dunn's multiple comparisons test. The soft PAAm gel was used as a control, and the protein was normalised against glyceraldehyde 3-phosphate dehydrogenase (GAPDH) or β-actin as the housekeeping protein. * indicate p< 0.05.

3.7.2 EMT proteins

The protein levels of TJP1(ZO1), as shown in Figures 15 D and F, showed a decrease in the medium (0.9±0.1) and rigid (0.7±0.5) hydrogels, respectively. The opposite trend was observed for E-CAD, where a significant increase ($p<0.05$) was observed on the rigid (1.9±0.7) gels, similar to the medium (1.4±0.5) gels, although not statistically significant. This increase could be an indication of increased cancer stemness, as high E-CAD expression was linked to increased cancer stemness (Lewis-Tuffin et al., 2010; Noronha et al., 2021). Furthermore, increased stiffness appears to promote EMT by causing an increase in mesenchymal proteins N-CAD and VIMENTIN, although not significant (Figures 16 B, C, F). N-CAD showed increased protein levels on the medium (1.3±0.3) and rigid (2.0±0.3) hydrogels, respectively. For VIMENTIN, the was increased on the rigid hydrogels (1.8±0.7). The protein level of TGF-ß, shown in Figures 16 E and F, showed an increase in medium (1.4±0.6) and rigid (1.5±0.5) hydrogels, respectively. This data could be an indicator that the cells are going through EMT, as it showed an increase in some mesenchymal proteins and a decrease in some epithelial proteins (Fang & Kang, 2021; Kröger et al., 2019; Lu & Kang, 2019).

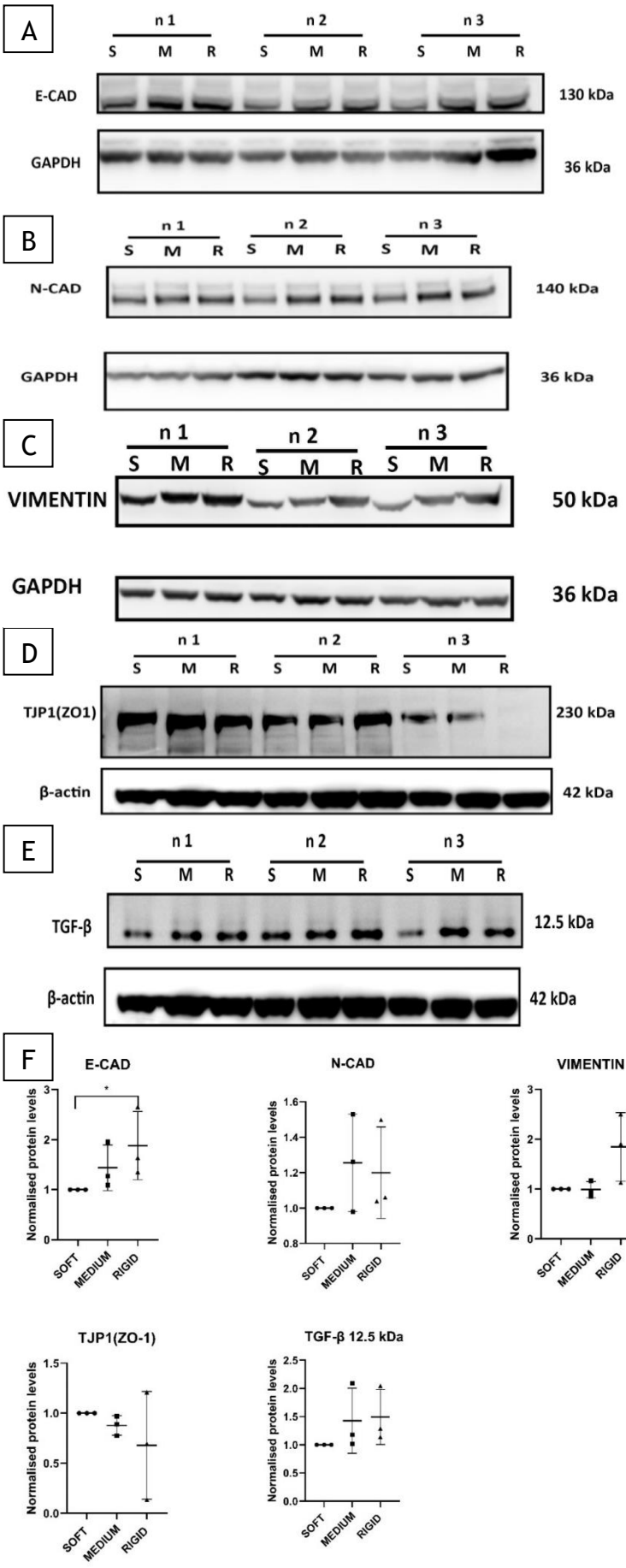
A
n 1
n 2
n 3
S M R S M R S M R
E-CAD
130 kDa
GAPDH
36 kDa
B
n 1
n 2
n 3
S M R S M R S M R
N-CAD
140 kDa
GAPDH
36 kDa
C
n 1
n 2
n 3
S M R S M R S M R
VIMENTIN
50 kDa
GAPDH
36 kDa
D
n 1
n 2
n 3
S M R S M R S M R
TJP1(ZO1)
230 kDa
β-actin
42 kDa
E
n 1
n 2
n 3
S M R S M R S M R
TGF-β
12.5 kDa
β-actin
42 kDa
F
E-CAD
N-CAD
VIMENTIN
TJP1(ZO-1)
TGF-β 12.5 kDa
Normalised protein levels
SOFT
MEDIUM
RIGID

Figure 17. Immunoblots quantification of EMT markers protein levels in response to the change in stiffness (n=3). (A-E) The immunoblots and the corresponding housekeeping protein used for quantification. (F) Quantification of E-CAD, N-CAD, VIMENTIN, TJP1(ZO-1) and TGF-β 12.5 kDa protein levels on the soft, medium and rigid hydrogels. Shapiro-Wilk normality test, Kruskal-Wallis test, followed by Dunn's multiple comparisons test. The soft PAAm gel was used as a control, and the protein was normalised against glyceraldehyde 3-phosphate dehydrogenase (GAPDH) or β-actin as the housekeeping protein. * indicate p< 0.05.

3.7.3 EMT Transcription Factors

There was a significant increase in levels of SNAI1(SNAIL) in response to the increased stiffness ($p<0.05$), as shown in Figures 18A and B, on medium (1.5±0.2) and rigid (1.4±0.15) hydrogels, respectively. This was a further indicator that the cells are going through EMT by losing their epithelial properties, which are repressed by SNAI1(SNAIL), and gaining mesenchymal properties promoted by it (De Herreros et al., 2010; Lamouille et al., 2014). This was consistent with EMT proteins data as it shows the same response to stiffness changes, where the medium and rigid gels had higher protein levels for mesenchymal markers and decreased levels of epithelial markers.

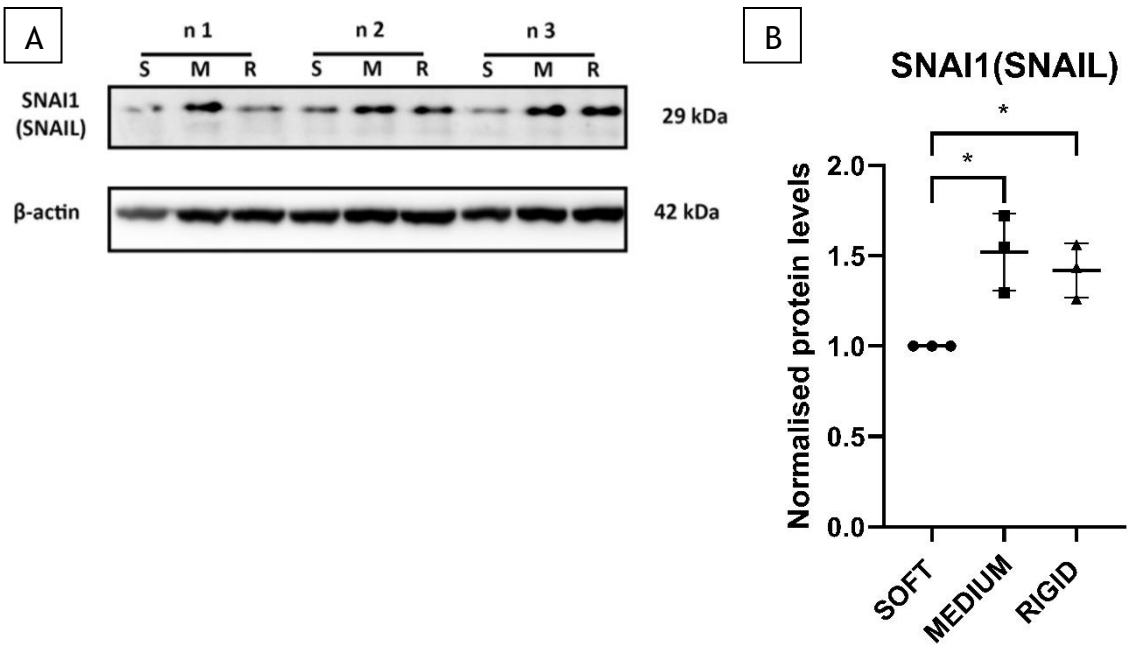

Figure 18. Immunoblots quantification of EMT transcription factor protein levels in response to stiffness change(n=3). (A) The immunoblots and the corresponding housekeeping proteins used for quantification. (B) Quantification of SNAI1(SNAIL) protein levels on the soft, medium and rigid hydrogels. Shapiro-Wilk normality test, Kruskal-Wallis test, followed by Dunn's multiple comparisons test. The soft PAAm gel was used as a control, and the protein was normalised against glyceraldehyde 3-phosphate dehydrogenase (GAPDH) or β-actin as the housekeeping protein. * indicate p< 0.05.

3.7.4 CSC Proteins

The following CSC proteins, SOX-2, ABCG2, and ALDH1A1, showed an increase in protein levels in response to stiffness (Figures 19 C, E, F and H). The protein levels of SOX-2 showed an increase in the medium (1.9±0.15) and rigid (3.2±3.4) hydrogels, respectively. The same trend was observed on the protein levels of ABCG2, where the medium and rigid protein levels were (1.4±0.4) and (1.3±0.4), respectively. For ALDH1A1, an increase was observed in the medium (2.6±1.7) and rigid (2.8±2.4) hydrogels, respectively. This could indicate that the cells are gaining Stem cell-like properties in response to the increased stiffness; however, the increase was not statistically significant.

A statistically significant increase in the protein levels of POU5F1(OCT-4) in medium and rigid gels compared to soft gels ($P<0.05$) is shown in Figures 19 D, H. The observed protein levels, medium and rigid, were (1.8±0.2) and (1.7±0.3), respectively. The increase in CSC properties is further illustrated by the increase in protein levels of EGFR in medium (1.2±0.11) compared to soft gels; however, it is not statistically significant, and the increase in protein level in rigid (1.3±0.16) compared to soft($P<0.05$).

Lastly, there was a notable increase in the protein levels of NESTIN and CD133, which are specific for GBM. In terms of protein levels of NESTIN, Figures 19A and H show a statistically significant increase in rigid (2.0±0.3) compared to medium and soft, being $P<0.01$ and $P<0.001$, respectively. For CD133, the protein levels showed an increase associated with the stiffness increase, where medium and rigid gels had a considerable increase compared to soft($P<0.0001$), as shown in Figures 19B and H. The observed protein levels on medium and rigid hydrogels were (5.3±0.8) and (5.1±0.14), respectively. This increase in protein levels of NESTIN and CD133 related to the increase in stiffness is a major indicator that these GBM cells gain CSC properties.

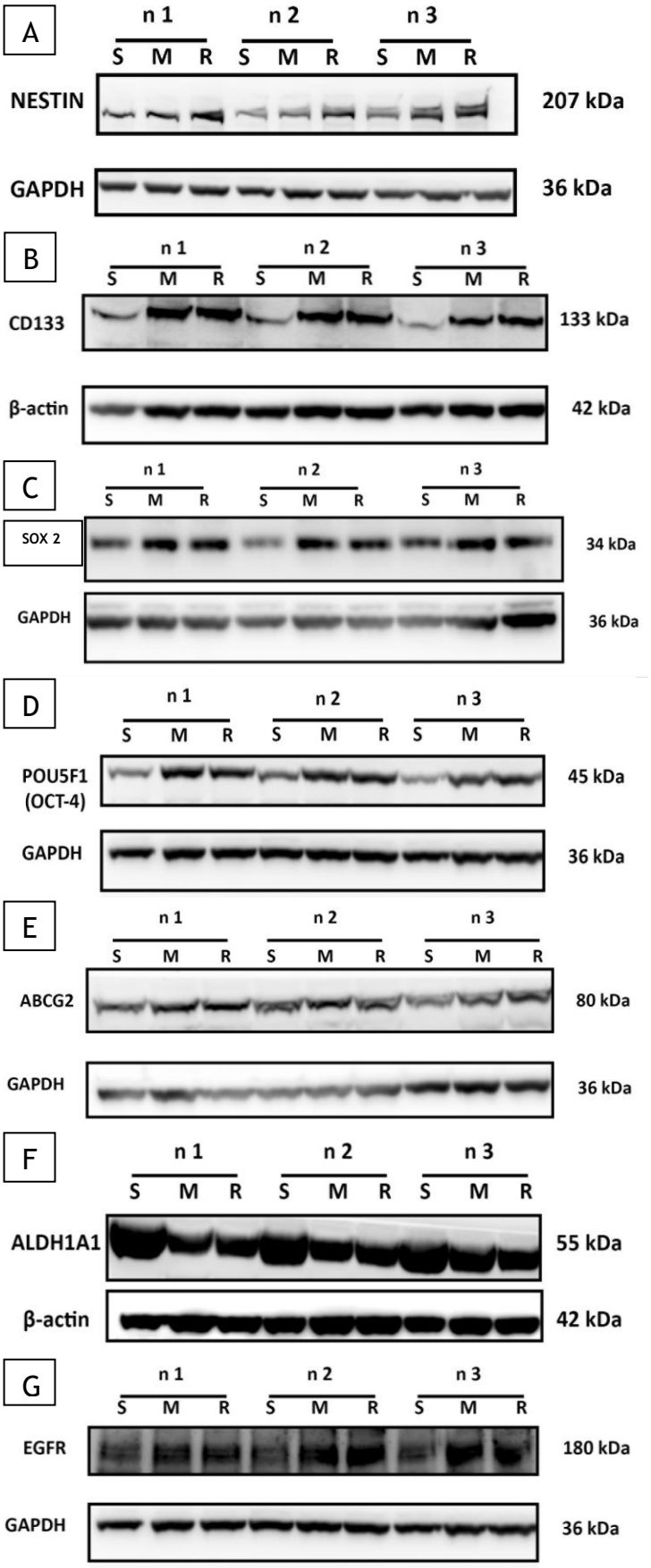
A
n 1
n 2
n 3
S M R S M R S M R
NESTIN
207 kDa
GAPDH
36 kDa
B
n 1
n 2
n 3
S M R S M R S M R
CD133
133 kDa
β-actin
42 kDa
C
n 1
n 2
n 3
S M R S M R S M R
SOX 2
34 kDa
GAPDH
36 kDa
D
n 1
n 2
n 3
S M R S M R S M R
POU5F1
(OCT-4)
45 kDa
GAPDH
36 kDa
E
n 1
n 2
n 3
S M R S M R S M R
ABCG2
80 kDa
GAPDH
36 kDa
F
n 1
n 2
n 3
S M R S M R S M R
ALDH1A1
55 kDa
β-actin
42 kDa
G
n 1
n 2
n 3
S M R S M R S M R
EGFR
180 kDa
GAPDH
36 kDa

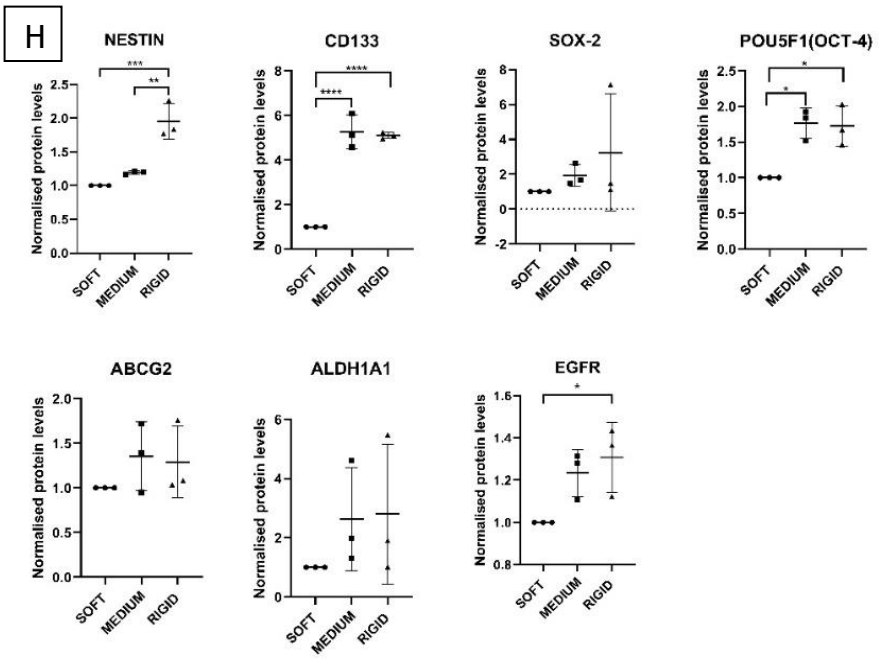

Figure 19. Immunoblots quantification of CSC markers protein levels in response to stiffness change(n=3). (A-G) The immunoblots and the corresponding housekeeping proteins used for quantification. (H) Quantification of NESTIN, CD133, SOX-2, POU5F1(OCT-4), ABCG2, ALDH1A1 and EGFR protein levels on the soft, medium and rigid Shapiro-Wilk normality test, Kruskal-Wallis test, followed by Dunn's multiple comparisons test. The soft PAAm gel was used as a control, and the protein was normalised against glyceraldehyde 3-phosphate dehydrogenase (GAPDH) or β-actin as the housekeeping protein. *, **, * and **** indicate p< 0.05, 0.01, 0.001 and 0.0001, respectively.**

4 Discussion

As the main aim of this project is to investigate how mechanical stiffness influences EMT and cancer stemness of GBM cells, PAAm hydrogels have been selected for their high tunability since they allow the production of hydrogels with a wide range of stiffness with consistent outcomes (Jafari et al., 2022; J. Lee et al., 2013; J. P. Lee et al., 2016; Xu et al., 2017). Therefore, we chose three relevant stiffnesses to GBM tumours: Soft 305.9±16.9Pa, Medium 10.5±0.4kPa, and rigid 34.9±5.1kPa. These stiffnesses were selected based on their potential impact on EMT and cancer stemness of GBM cells, a key focus of this study. Although the hydrogel stiffness was consistently reproducible, the use of 50mm coverslips raised concerns about the homogeneity of their stiffness as the cell response was different compared to 30mm hydrogels. The 50mm coverslips were fabricated to increase the yield of proteins when extracting, as they would reduce the time, costs, and workload associated with functionalising and cell culture. Due to the size of the gels, measuring the stiffness using rheology would require large volumes, which was overcome by using lower volumes and measuring them using nanoindentation. Another concern was what is the appropriate volume to use for the 50mm. This was validated through nanoindentation where two volumes of the same hydrogel mixture were used to compare two hydrogels of the same stiffness as the soft gels of the two volumes, with 50 and 100µL different stiffness of 140.3 ±6.0Pa and 321.7±59.8 Pa, respectively. For medium, the lower volume had a much higher stiffness of 24.54±5.8kPa, and the higher volume stiffness was 8.01±0.4kPa. The same observation was made on the rigid hydrogels in the two volumes, with their stiffness being 44.15±3.4kPa and 39.19±2.6kPa, respectively. The larger volumes used give more consistent stiffness that is correlated with rheology data; this could be a result of contact between the Nanoindenter and the coverslip where the probe is in contact with the glass coverslip, which interferes with the measurement, giving higher stiffness values; however, it is unclear why the lower volume stiffness measurement was lower for the soft hydrogels. The 50mm hydrogels were fabricated late in this project; thus, they were not used in any of the experiments.

As the PAAm hydrogels are bioinert and do not promote cell adhesion, thus their biochemical properties should be modified before biomedical applications

(Gribova et al., 2011). For the soft PAAm hydrogels, the cells do not attach or spread on the surface of the control (bare hydrogel) due to the lack of ligands to promote cell-material interactions, whereas only collagen Type I allowed them to attach and spread. The same observation was made on the medium PAAm hydrogels, as only collagen type I promoted cell attachment and spreading. However, a notable observation was made on the rigid PAAm hydrogels where cell attachment was seen on the control sample (Bare hydrogel), which can be attributed to the high stiffness, and the same observation was made on the sulfo-SANPAH sample. Collagen type I showed the same response on rigid, medium and soft hydrogels where a high number of cells attached and spread. This can be attributed to the high concentration of collagen type I used. Multiple concentrations of collagen type I were used to minimise the influence of available binding domains, and it was observed that 20 and 40 µg/mL showed similar cell morphology and number of cells. These two concentrations of 20 and 40 µg/mL of collagen type I showed significant differences in the ligand density for the three stiffnesses, implying that the cellular response only attributed to the stiffness and not ligand density as a high ligand density would have the same morphology of as the stiff hydrogels (Stanton et al., 2019). Following the assessment of the ligand density, YAP localisation was investigated to assess whether cells can sense the stiffness of the hydrogels. It has been identified that the Transcriptional regulator Yorkie-homologue YAP (Yes-associated protein) is a mechanical rheostat, where its localisation correlates with ECM stiffness for high-stiffness YAP will translocate to the nuclease. The results described above showed that YAP was observed in the cell's cytoplasm on the soft hydrogels. As the stiffness increases, higher amounts of YAP translocate to the nuclease, indicating the cell can sense and respond to the hydrogels' stiffness but not to the ligand density, as it has been demonstrated that the three-stiffness had no significant difference in the ligand density. Although the ligand density and stiffness play a major role in influencing cellular response, it can also be influenced by other factors, such as the nanotopography of the different hydrogel stiffnesses, where it was shown to influence cell morphology and adhesion by interacting with integrin receptors which intern impacts cell function, growth, differentiation and modulating signalling pathways altering processes like gene expression and cytoskeletal organization (Dalby et al., 2014; D. H. Kim et al., 2012; Luo et al., 2022). Another factor is the porosity, as the different stiffnesses of PAAm hydrogels have different pore sizes, as

demonstrated by previous studies, which can influence cell migration, mechanical properties and differentiation(Chighizola et al., 2019; Hadden et al., 2017). Thus, the influence of these factors on glioblastoma cells should be investigated to assess whether they influence the response observed.

Mechanical properties can influence GBM cell behaviour as it has been shown that highly invasive GBM can generate higher forces on the substrate and are much stiffer, increasing mobility and invasiveness(Monzo et al., 2021). For the cell to respond to mechanical stresses, the biochemical signals are translated via sensor molecules in a process known as mechanotransduction. The remodelling of the actin cytoskeleton is regulated by Rho-family small GTPases, which include RhoA that is activated via mechanical stresses by affecting the downstream proteins like pMLC2 (Birukov et al., 2003; Kaunas et al., 2005; Ohashi et al., 2017). One of these downstream proteins is Rho-associated coiled-coil forming kinase (ROCK), which affects crucial functions such as proliferation, secretion and motility (Amano et al., 2010; Maekawa et al., 1999; McBeath et al., 2004; Riento & Ridley, 2003). It also controls the organisation and stabilisation of the actin filaments by phosphorylating some proteins like myosin light chain (MLC) (Qiao et al., 2014; Totsukawa et al., 2000). The phosphorylation of MLC2 enhances cell contractility, which is essential for promoting cell migration and invasion (Oh et al., 2023). The gene expression levels were studied to demonstrate that the change in stiffness alters the expression of RhoA, ROCK1 and ROCK2, where they destabilise and stabilise the actin cytoskeleton(Maekawa et al., 1999). Although there was an increase in the gene expression of the RhoA, ROCK1, and ROCK2, it was not significant; it still illustrated the main point, where medium and rigid hydrogels had higher gene expression than soft hydrogels. The protein levels data also supported this as the same response was observed, with a slight increase in protein levels of pMLC2 and VINCULIN on medium and rigid. Furthermore, there was a significant increase in ROCK1 protein levels in the medium ($P<0.05$) and a slight increase in the rigid hydrogels, illustrating how the stiffness influenced mechanotransduction proteins in GBM cells.

Integrin gene expression has been investigated due to its relation to mechanotransduction signalling (J. H. C. Wang, 2006). It has been proposed that integrins are mechanosensors (Campbell & Humphries, 2011). Two trends were

observed: the following integrins, ITGß3, ITGß4, ITGß5, and ITGα5, were downregulated in response to an increase in the stiffness. However, the downregulation was not significant. This could be attributed to the high stiffness activating mechanotransduction pathways and down-regulating integrin expressions as part of the feedback mechanism to maintain and modulate cell adhesion (Levental et al., 2009; M. Li et al., 2021). These integrins were shown in previous studies to be upregulated in GBM as the debases progress(Delamarre et al., 2009; Ellert-Miklaszewska et al., 2020; Gingras et al., 1995; Thorén et al., 2019; Verhaak et al., 2010). While the following integrin genes were upregulated ITGß1, ITGß7, ITGα1, and ITGαv, although no statistically significant difference was found, the increase of expression of these integrins could be a result of the increase in the mechanotransduction event and the cellular adhesion modulation (Levental et al., 2009; M. Li et al., 2021). This was consistent with previous studies that showed similar gene expression changes in GBM cells(Delamarre et al., 2009; Ellert-Miklaszewska et al., 2020; Gingras et al., 1995). The data indicates that mechanical stiffness influenced changes in the integrins gene expression. Studying them at the protein level would be interesting due to their fundamental role in force transmission and microenvironment sensing. This data also correlates with the mechanotransduction genes and proteins previously studied, where the mechanotransduction signalling increases as the stiffness increases (Sun et al., 2016).

In EMT, cells acquire a migratory mesenchymal phenotype and lose their epithelial properties (Nieto et al., 2016); it is also regulated by the physical microenvironment (Gomez et al., 2010). The following set of experiments investigated the influence of stiffness on EMT markers and how these common markers in these cells would respond to a change in stiffness. E-CAD is an epithelial marker which is involved in cell-to-cell junctions, and it is downregulated when cells are undergoing EMT (Zeisberg & Neilson, 2009); TJP1(ZO1) tight junction protein, another epithelial marker crucial for maintaining epithelial cell morphology that is also downregulated during EMT and the disruption tight Junction complex promotes invasion and metastasis (Bhat et al., 2019; Georgiadis et al., 2010; Y. E. Kim et al., 2019). Vinculin, an epithelial marker, is also downregulated during EMT (T. Li et al., 2014). The expression of VINCULIN and TJP1(ZO-1) was down-regulated in response to the increased stiffness, indicating

that the cells are losing epithelial characteristics. This was further illustrated by the protein levels of TJP1(ZO-1), as medium and rigid hydrogels had lower protein levels compared to soft ones. However, E-CAD gene expression has been upregulated in the medium and rigid hydrogels, and there was a significant increase in the protein levels in the rigid ($P<0.05$) hydrogels compared to soft ones; a similar increase was observed in the medium hydrogels compared to soft ones, although it was not statistically significant. This increased E-CAD expression could indicate an increase in cancer stemness as it has been associated with increased cancer stemness capabilities (Lewis-Tuffin et al., 2010; Noronha et al., 2021). This might not contradict the other data for the epithelial markers as not all EMT markers would show the same response to stiffness due to EMT being a dynamic process with an intermediate stage, which could explain this phenomenon (Leggett et al., 2021).

Mesenchymal markers like N-CAD, vimentin, FN and TGF-ß are upregulated during EMT (Y. E. Kim et al., 2019; Park & Schwarzbauer, 2014). TGF-ß is a well-known promoter of EMT, which regulates the transcription of epithelial and mesenchymal proteins influencing cell-cell junction and migration capabilities (Lamouille et al., 2014; Xu et al., 2009). This was not the case, as gene expression data for N-CAD, FN, and TGF-ß were slightly down-regulated in response to stiffness increase, and a significant decrease in VIMENTIN gene expression was observed on the medium ($P<0.05$) and rigid ($P<0.01$) hydrogels. However, the protein levels were completely opposite to the gene expression data; an increase in the protein levels of VIMENTIN, N-CAD and TGF-ß was observed on the medium and rigid hydrogels. This showed the expected trends and is more relevant as proteins are the functional units of the cells and are more reliable in this context. This further indicates that the cells might be in a partial EMT state, losing some epithelial characteristics and gaining some mesenchymal characteristics. Another explanation is that increased protein levels could lead to down-regulation of the gene through a negative feedback loop to maintain cellular balance by preventing the protein from accumulating excessively(J. Kim et al., 2020).

For the cells to go through EMT, the epithelial markers like E-CAD are firstly suppressed, and the mesenchymal markers like vimentin are induced by the EMT transcription factors (Leggett et al., 2021). These EMT transaction factors include

SNAI1(Snail) and SNAI2(Slug) members of the snail family, which play a major role in GBM progression (Du et al., 2017). Other transcription factors are Twist, ZEB1 and ZEB2, which are responsible for mesenchymal change promoting the invasion of GBM (Mikheeva et al., 2010; Poonaki et al., 2022). To illustrate further that the cells underwent EMT, the following EMT transcription factors, SNAI1 (snail), SNAI2 (slug), Twist, ZEB1, and ZEB1, were investigated. The gene expression of SNAI2 (slug) and ZEB1 have been slightly downregulated due to stiffness, and ZEB2 was upregulated in the medium and downregulated in the rigid hydrogels. The same trend was observed for the gene expression for SNAI1(SNAIL) as it has been downregulated on the medium and rigid; however, at the protein level, it has been significantly increased on medium and rigid hydrogels in response to stiffness, further illustrating the data at the protein level is more relevant in this case as protein are what drive changes in the cells.

The formation of solid tumours, which are stiffer than normal tissue, is part of the cancer progression (Imbault et al., 2017; Miroshnikova et al., 2016). As the GBM progresses, the stiffness increases, facilitating EMT and invasion. It remains challenging to draw a definitive conclusion due to the limitations of the time point used for the qPCR data that has been analysed. However, the positive trends observed in both EMT and EMT transcription factor data implied that the high stiffness promoted GBM cells to undergo EMT to gain migratory capability and facilitate invasion. This was highlighted by enhancement in the integrin mechanosignalling, which has been linked to increased invasion, treatment resistance and survival as stiffer ECM and increased tissue tension were linked to elevated integrin mechanosignalling promoting mesenchymal phenotype (Barnes et al., 2018).

There might be several possible reasons why no conclusive conclusions were drawn from the qPCR finding. The first is that the time point selected for the experiments did not align with the time point in which the stiffness induced the cells to express the genes of interest. Another probable reason would be that the cell density was high enough to allow the cells to sense neighbouring cells, thus reducing gene expression.

CSCs play an essential role in the ability of cancer cells to gain renewal abilities and increase their regeneration potential; this also enhances the resistance of

cancer cells to therapy. All of this is driven by the CSC markers that are not expressed in the normal tissue (Al-Hajj et al., 2003b; Bonnet & Dick, 1997; Gupta et al., 2009). The following markers, NESTIN, a marker specific to GBM that has been shown to promote tumour growth, relapse and therapy resistance, and CDC42, closely related to invasiveness potential and migration, showed an increase due to stiffness although not statistically significant, this implied that the increased stiffness promoted cancer stemness (Shafi & Siddiqui, 2022; Zhong et al., 2021). This was contradicted by ALDH1A1's significant decrease in expression ($p<0.001$), which was associated with therapeutic resistance in brain cancer (Wu et al., 2022). The POU5F1(OCT-4) and sox-2, transcription factors that maintain stemness and promote invasion, showed an increased expression and gained cancer stemness capability associated with the change in stiffness (Ma et al., 2021; Yue et al., 2022). Furthermore, this is supported by the significant increase in expression of the CXCR4 ($P<0.05$), which plays a major role in the cell's survival, migration and proliferation and ABCG2 ($P<0.05$), which is responsible for self-renewal properties and therapeutic resistance and tumour initiation (Raguž et al., 2024; Würth et al., 2014). The same trends were observed on the protein level of SOX-2 and ABCG-2, where the protein levels increased in response to stiffness. There was a significant increase of POU5F1 (OCT-4) protein levels in medium ($P<0.05$) and rigid ($P<0.05$) hydrogels compared to soft. Epidermal growth factor receptor (EGFR) is a protein that contributes to GBM progression and tumorigenesis (Brennan et al., 2013; Oprita et al., 2021). There was a significant increase in EGFR protein levels in the rigid ($P<0.05$) hydrogels compared to soft, and a similar increase was observed in the medium compared to soft; however, it was not significant. The protein levels of ALDH1A1 showed the opposite trend to the gene expression, where there were increased protein levels in response to stiffness. This could be a result of the negative feedback loop to prevent the accumulation of this protein (J. Kim et al., 2020). CD133 is a CSC marker specific to GBM and associated with therapy resistance, poor prognosis, and tumour recurrence (Joyce et al., 2023; Mia-Jan et al., 2013). There was a significant increase in the protein levels of NESTIN ($P<0.001$) and CD133 ($P<0.0001$) as the stiffness increased, indicating an increase in CSC capabilities. As the medium and rigid hydrogels were chosen to recapitulate the stiffness of GBM tumours, it was shown that the stiffness promoted cancer stemness. This was suggested by increased gene expression of NESTIN, CDC42, CXCR4, SOX-2, OCT-4 and ABCG2 and

increased protein levels of NESTIN, CD133, SOX-2, OCT-4, ABCG2, EGFR and ALDH1A1.

The use of primary cells in this project makes these results reliable as they exhibit tumour heterogeneity and preserve the genetic and molecular background of the individual, accurately representing disease. A lot of research has been conducted on GBM cell lines, which showed similar trends as the cell lines were restricted on soft substrates and showed stiffens-dependent migration(Ananthanarayanan et al., 2011; Grundy et al., 2016; Ulrich et al., 2009). GBM cell lines were used in other studies, but many limitations are associated with their use. The first is the limited recapitulation of the genetic and epigenetic diversity in a patient tumour and the tumour heterogeneity, which could result in findings not fully translating to clinical outcomes (Hynds et al., 2018). Factors like passage number, culture conditions and genetic drift contribute to variability in the results, leading to irresectability and inconsistencies for data obtained between different laboratories (Pollak et al., 2021). Other factors, such as long-term, can strain cell lines differently to diverge genetically and phenotypically, influencing the reproducibility and cell response (Hynds et al., 2018)

5 Conclusion

The results showed how influential mechanical stiffness is on the cellular response of GBM cells. The increased stiffness alters the gene expression and protein levels of GBM cells, correlated with increased levels of mechanotransduction of genes and proteins, showing that hydrogels were able to initiate mechanotransduction events illustrated by the change in gene and protein levels of RhoA, ROCK1, ROCK2 and pMLC2. For stiffnesses similar to GBM tumours, EMT has been promoted compared to the stiffness of the normal brain tissue indicated by the increased protein levels of N-CAD, Vimentin, TGF-β 12.5kDa and the decrease in the protein levels of TJP1(ZO-1), allowing the cells to migrate and invade. Cancer stemness markers were increased in the stiffnesses comparable to GBM tumours stiffness as demonstrated by the increase in the gene expression of NESTIN, CXCR4, ABCG2 and the protein levels of NESTIN, CD133, POU5F1(Oct-4) and EGFR. Mechanical stiffness appears to be crucial in promoting EMT and cancer stemness, confirming that increased stiffness promotes invasion capabilities in GBM.

6 Future work

Based on the findings of this research, further work is required in order to advance this field. The Real-time qPCR experiment should be performed at an earlier time point to detect the changes in gene expression. Furthermore, the significant changes should be studied at the protein level following the gene expression experiments. They would allow for relations between cancer stemness and EMT to be extensively investigated.

References

Abraham, B. K., Fritz, P., McClellan, M., Hauptvogel, P., Athelogou, M., & Brauch, H. (2005). Prevalence of CD44+/CD24-/low cells in breast cancer may not be associated with clinical outcome but may favor distant metastasis. *Clinical Cancer Research*, *11*(3). https://doi.org/10.1158/1078-0432.1154.11.3

Acharekar, A., Bachal, K., Shirke, P., Thorat, R., Banerjee, A., Gardi, N., Majumder, A., & Dutt, S. (2023). Substrate stiffness regulates the recurrent glioblastoma cell morphology and aggressiveness: Recurrent GBM have differential mechanosignaling response. *Matrix Biology*, *115*. https://doi.org/10.1016/j.matbio.2022.12.002

Al-Hajj, M., Wicha, M. S., Benito-Hernandez, A., Morrison, S. J., & Clarke, M. F. (2003a). Prospective identification of tumorigenic breast cancer cells. *Proceedings of the National Academy of Sciences*, *100*(7), 3983–3988.

Al-Hajj, M., Wicha, M. S., Benito-Hernandez, A., Morrison, S. J., & Clarke, M. F. (2003b). Prospective identification of tumorigenic breast cancer cells. *Proceedings of the National Academy of Sciences of the United States of America*, *100*(7). https://doi.org/10.1073/pnas.0530291100

Amano, M., Nakayama, M., & Kaibuchi, K. (2010). Rho-kinase/ROCK: A key regulator of the cytoskeleton and cell polarity. In *Cytoskeleton* (Vol. 67, Issue 9). https://doi.org/10.1002/cm.20472

An, Y., & Ongkeko, W. M. (2009). ABCG2: The key to chemoresistance in cancer stem cells? In *Expert Opinion on Drug Metabolism and Toxicology* (Vol. 5, Issue 12). https://doi.org/10.1517/17425250903228834

Ananthanarayanan, B., Kim, Y., & Kumar, S. (2011). Elucidating the mechanobiology of malignant brain tumors using a brain matrix-mimetic hyaluronic acid hydrogel platform. *Biomaterials*, *32*(31). https://doi.org/10.1016/j.biomaterials.2011.07.005

Ansieau, S., Collin, G., & Hill, L. (2014). EMT or EMT-promoting transcription factors, where to focus the light? *Frontiers in Oncology*, *4*(NOV). https://doi.org/10.3389/fonc.2014.00353

Baker, B. M., & Chen, C. S. (2012). Deconstructing the third dimension-how 3D culture microenvironments alter cellular cues. In *Journal of Cell Science* (Vol. 125, Issue 13). https://doi.org/10.1242/jcs.079509

Barnes, J. M., Kaushik, S., Bainer, R. O., Sa, J. K., Woods, E. C., Kai, F. B., Przybyla, L., Lee, M., Lee, H. W., Tung, J. C., Maller, O., Barrett, A. S., Lu, K. V., Lakins, J. N., Hansen, K. C., Obernier, K., Alvarez-Buylla, A., Bergers, G., Phillips, J. J., … Weaver, V. M. (2018). A tension-mediated glycocalyx–integrin feedback loop promotes mesenchymal-like glioblastoma. *Nature Cell Biology*, *20*(10). https://doi.org/10.1038/s41556-018-0183-3

Barnes, J. M., Przybyla, L., & Weaver, V. M. (2017). Tissue mechanics regulate brain development, homeostasis and disease. In *Journal of Cell Science* (Vol. 130, Issue 1). https://doi.org/10.1242/jcs.191742

Behin, A., Hoang-Xuan, K., Carpentier, A. F., & Delattre, J. Y. (2003). Primary brain tumours in adults. In *Lancet* (Vol. 361, Issue 9354). https://doi.org/10.1016/S0140-6736(03)12328-8

Beningo, K. A., Lo, C. M., & Wang, Y. L. (2002). Flexible polyacrylamide substrata for the analysis of mechanical interactions at cell-substratum adhesions. In *Methods in Cell Biology* (Vol. 2002, Issue 69). https://doi.org/10.1016/S0091-679X(02)69021-1

Bhargav, A. G., Domino, J. S., Chamoun, R., & Thomas, S. M. (2022). Mechanical Properties in the Glioma Microenvironment: Emerging Insights and Theranostic Opportunities. In *Frontiers in Oncology* (Vol. 11). https://doi.org/10.3389/fonc.2021.805628

Bhat, A. A., Uppada, S., Achkar, I. W., Hashem, S., Yadav, S. K., Shanmugakonar, M., Al-Naemi, H. A., Haris, M., & Uddin, S. (2019). Tight junction proteins and signaling pathways in cancer and inflammation: A functional crosstalk. In *Frontiers in Physiology* (Vol. 10, Issue JAN). https://doi.org/10.3389/fphys.2018.01942

Birukov, K. G., Jacobson, J. R., Flores, A. A., Ye, S. Q., Birukova, A. A., Verin, A. D., & Garcia, J. G. N. (2003). Magnitude-dependent regulation of pulmonary endothelial cell barrier function by cyclic stretch. *American Journal of Physiology - Lung Cellular and Molecular Physiology*, *285*(4 29-4). https://doi.org/10.1152/ajplung.00336.2002

Bonnet, D., & Dick, J. E. (1997). Human acute myeloid leukemia is organized as a hierarchy that originates from a primitive hematopoietic cell. *Nature Medicine*, *3*(7). https://doi.org/10.1038/nm0797-730

Boutet, A., De Frutos, C. A., Maxwell, P. H., Mayol, M. J., Romero, J., & Nieto, M. A. (2006). Snail activation disrupts tissue homeostasis and induces fibrosis in the adult kidney. *EMBO Journal*, *25*(23). https://doi.org/10.1038/sj.emboj.7601421

Brennan, C. W., Verhaak, R. G. W., McKenna, A., Campos, B., Noushmehr, H., Salama, S. R., Zheng, S., Chakravarty, D., Sanborn, J. Z., Berman, S. H., Beroukhim, R., Bernard, B., Wu, C. J., Genovese, G., Shmulevich, I., Barnholtz-Sloan, J., Zou, L., Vegesna, R., Shukla, S. A., … McLendon, R. (2013). The somatic genomic landscape of glioblastoma. *Cell*, *155*(2). https://doi.org/10.1016/j.cell.2013.09.034

Brodbelt, A., Greenberg, D., Winters, T., Williams, M., Vernon, S., & Collins, V. P. (2015). Glioblastoma in England: 2007-2011. *European Journal of Cancer*, *51*(4). https://doi.org/10.1016/j.ejca.2014.12.014

Burdett, E., Kasper, F. K., Mikos, A. G., & Ludwig, J. A. (2010). Engineering tumors: A tissue engineering perspective in cancer biology. In *Tissue Engineering - Part B: Reviews* (Vol. 16, Issue 3). https://doi.org/10.1089/ten.teb.2009.0676

Butcher, D. T., Alliston, T., & Weaver, V. M. (2009). A tense situation: Forcing tumour progression. In *Nature Reviews Cancer* (Vol. 9, Issue 2). https://doi.org/10.1038/nrc2544

Campbell, I. D., & Humphries, M. J. (2011). Integrin structure, activation, and interactions. In *Cold Spring Harbor Perspectives in Biology* (Vol. 3, Issue 3). https://doi.org/10.1101/cshperspect.a004994

Castanon, I., & Baylies, M. K. (2002). A Twist in fate: Evolutionary comparison of Twist structure and function. *Gene*, *287*(1–2). https://doi.org/10.1016/S0378-1119(01)00893-9

Cawkill, D., & Eaglestone, S. S. (2007). Evolution of cell-based reagent provision. In *Drug Discovery Today* (Vol. 12, Issues 19–20). https://doi.org/10.1016/j.drudis.2007.08.014

Chauvet, D., Imbault, M., Capelle, L., Demene, C., Mossad, M., Karachi, C., Boch, A. L., Gennisson, J. L., & Tanter, M. (2016). In Vivo Measurement of

Brain Tumor Elasticity Using Intraoperative Shear Wave Elastography. *Ultraschall in Der Medizin*, *37*(6). https://doi.org/10.1055/s-0034-1399152

Chighizola, M., Dini, T., Lenardi, C., Milani, P., Podestà, A., & Schulte, C. (2019). Mechanotransduction in neuronal cell development and functioning. In *Biophysical Reviews* (Vol. 11, Issue 5). https://doi.org/10.1007/s12551-019-00587-2

Choi, Y., Lee, H. J., Jang, M. H., Gwak, J. M., Lee, K. S., Kim, E. J., Kim, H. J., Lee, H. E., & Park, S. Y. (2013). Epithelial-mesenchymal transition increases during the progression of in situ to invasive basal-like breast cancer. *Human Pathology*, *44*(11). https://doi.org/10.1016/j.humpath.2013.07.003

da Silva-Diz, V., Lorenzo-Sanz, L., Bernat-Peguera, A., Lopez-Cerda, M., & Muñoz, P. (2018). Cancer cell plasticity: Impact on tumor progression and therapy response. In *Seminars in Cancer Biology* (Vol. 53). https://doi.org/10.1016/j.semcancer.2018.08.009

Dalby, M. J., Gadegaard, N., & Oreffo, R. O. C. (2014). Harnessing nanotopography and integrin-matrix interactions to influence stem cell fate. *Nature Materials*, *13*(6). https://doi.org/10.1038/nmat3980

De Herreros, A. G., Peiró, S., Nassour, M., & Savagner, P. (2010). Snail family regulation and epithelial mesenchymal transitions in breast cancer progression. In *Journal of Mammary Gland Biology and Neoplasia* (Vol. 15, Issue 2). https://doi.org/10.1007/s10911-010-9179-8

Delamarre, E., Taboubi, S., Mathieu, S., Bérenguer, C., Rigot, V., Lissitzky, J. C., Figarella-Branger, D., Ouafik, L., & Luis, J. (2009). Expression of integrin α6β1 enhances tumorigenesis in glioma cells. *American Journal of Pathology*, *175*(2). https://doi.org/10.2353/ajpath.2009.080920

Deng, B., Zhao, Z., Kong, W., Han, C., Shen, X., & Zhou, C. (2022). Biological role of matrix stiffness in tumor growth and treatment. In *Journal of Translational Medicine* (Vol. 20, Issue 1). https://doi.org/10.1186/s12967-022-03768-y

Dirks, P. B. (2008). Brain tumour stem cells: The undercurrents of human brain cancer and their relationship to neural stem cells. In *Philosophical Transactions of the Royal Society B: Biological Sciences* (Vol. 363, Issue 1489). https://doi.org/10.1098/rstb.2006.2017

Du, L., Tang, J. H., Huang, G. H., Xiang, Y., & Lv, S. Q. (2017). The progression of epithelial-mesenchymal transformation in gliomas. In *Chinese Neurosurgical Journal* (Vol. 3, Issue 1). https://doi.org/10.1186/s41016-017-0086-3

Elias, M. C., Tozer, K. R., Silber, J. R., Mikheeva, S., Deng, M., Morrison, R. S., Manning, T. C., Silbergeld, D. L., Glackin, C. A., Reh, T. A., & Rostomily, R. C. (2005). TWIST is expressed in human gliomas and promotes invasion. *Neoplasia*, *7*(9). https://doi.org/10.1593/neo.04352

Ellert-Miklaszewska, A., Poleszak, K., Pasierbinska, M., & Kaminska, B. (2020). Integrin signaling in glioma pathogenesis: From biology to therapy. In *International Journal of Molecular Sciences* (Vol. 21, Issue 3). https://doi.org/10.3390/ijms21030888

Fang, C., & Kang, Y. (2021). E-Cadherin: Context-Dependent Functions of a Quintessential Epithelial Marker in Metastasis. *Cancer Research*, *81*(23). https://doi.org/10.1158/0008-5472.CAN-21-3302

Franze, K. (2013). The mechanical control of nervous system development. *Development (Cambridge)*, *140*(15). https://doi.org/10.1242/dev.079145

Georgiadis, A., Tschernutter, M., Bainbridge, J. W. B., Balaggan, K. S., Mowat, F., West, E. L., Munro, P. M. G., Thrasher, A. J., Matter, K., Balda, M. S., &

Ali, R. R. (2010). The tight junction associated signalling proteins ZO-1 and ZONAB regulate retinal pigment epithelium homeostasis in mice. *PLoS ONE*, *5*(12). https://doi.org/10.1371/journal.pone.0015730

Ginestier, C., Hur, M. H., Charafe-Jauffret, E., Monville, F., Dutcher, J., Brown, M., Jacquemier, J., Viens, P., Kleer, C. G., Liu, S., Schott, A., Hayes, D., Birnbaum, D., Wicha, M. S., & Dontu, G. (2007). ALDH1 Is a Marker of Normal and Malignant Human Mammary Stem Cells and a Predictor of Poor Clinical Outcome. *Cell Stem Cell*, *1*(5). https://doi.org/10.1016/j.stem.2007.08.014

Gingras, M. claude, Roussel, E., Bruner, J. M., Branch, C. D., & Moser, richard P. (1995). Comparison of cell adhesion molecule expression between glioblastoma multiforme and autologous normal brain tissue. *Journal of Neuroimmunology*, *57*(1–2). https://doi.org/10.1016/0165-5728(94)00178-Q

Gomez, E. W., Chen, Q. K., Gjorevski, N., & Nelson, C. M. (2010). Tissue geometry patterns epithelial-mesenchymal transition via intercellular mechanotransduction. *Journal of Cellular Biochemistry*, *110*(1). https://doi.org/10.1002/jcb.22545

Gribova, V., Crouzier, T., & Picart, C. (2011). A material's point of view on recent developments of polymeric biomaterials: Control of mechanical and biochemical properties. In *Journal of Materials Chemistry* (Vol. 21, Issue 38). https://doi.org/10.1039/c1jm11372k

Griffith, L. G., & Swartz, M. A. (2006). Capturing complex 3D tissue physiology in vitro. In *Nature Reviews Molecular Cell Biology* (Vol. 7, Issue 3). https://doi.org/10.1038/nrm1858

Grundy, T. J., De Leon, E., Griffin, K. R., Stringer, B. W., Day, B. W., Fabry, B., Cooper-White, J., & O'Neill, G. M. (2016). Differential response of patient-derived primary glioblastoma cells to environmental stiffness. *Scientific Reports*, *6*. https://doi.org/10.1038/srep23353

Gunasinghe, N. P. A. D., Wells, A., Thompson, E. W., & Hugo, H. J. (2012). Mesenchymal-epithelial transition (MET) as a mechanism for metastatic colonisation in breast cancer. *Cancer and Metastasis Reviews*, *31*(3–4). https://doi.org/10.1007/s10555-012-9377-5

Gupta, P. B., Onder, T. T., Jiang, G., Tao, K., Kuperwasser, C., Weinberg, R. A., & Lander, E. S. (2009). Identification of Selective Inhibitors of Cancer Stem Cells by High-Throughput Screening. *Cell*, *138*(4). https://doi.org/10.1016/j.cell.2009.06.034

Hadden, W. J., Young, J. L., Holle, A. W., McFetridge, M. L., Kim, D. Y., Wijesinghe, P., Taylor-Weiner, H., Wen, J. H., Lee, A. R., Bieback, K., Vo, B. N., Sampson, D. D., Kennedy, B. F., Spatz, J. P., Engler, A. J., & Cho, Y. S. (2017). Stem cell migration and mechanotransduction on linear stiffness gradient hydrogels. *Proceedings of the National Academy of Sciences of the United States of America*, *114*(22). https://doi.org/10.1073/pnas.1618239114

Hamburger, A. W., & Salmon, S. E. (1977). Primary bioassay of human tumor stem cells. *Science*, *197*(4302). https://doi.org/10.1126/science.560061

Harrison, R. G., Greenman, M. J., Mall, F. P., & Jackson, C. M. (1907). Observations of the living developing nerve fiber. *The Anatomical Record*, *1*(5). https://doi.org/10.1002/ar.1090010503

Hemmati, H. D., Nakano, I., Lazareff, J. A., Masterman-Smith, M., Geschwind, D. H., Bronner-Fraser, M., & Kornblum, H. I. (2003). Cancerous stem cells can arise from pediatric brain tumors. *Proceedings of the National Academy*

of Sciences of the United States of America, *100*(25). https://doi.org/10.1073/pnas.2036535100

Hickman, J. A., Graeser, R., de Hoogt, R., Vidic, S., Brito, C., Gutekunst, M., van der Kuip, H., & Imi Predect consortium. (2014). Three-dimensional models of cancer for pharmacology and cancer cell biology: Capturing tumor complexity in vitro/ex vivo. In *Biotechnology Journal* (Vol. 9, Issue 9). https://doi.org/10.1002/biot.201300492

Hollier, B. G., Evans, K., & Mani, S. A. (2009). The epithelial-to-mesenchymal transition and cancer stem cells: A coalition against cancer therapies. In *Journal of Mammary Gland Biology and Neoplasia* (Vol. 14, Issue 1). https://doi.org/10.1007/s10911-009-9110-3

Hutmacher, D. W. (2010). Biomaterials offer cancer research the third dimension. In *Nature Materials* (Vol. 9, Issue 2). https://doi.org/10.1038/nmat2619

Hynds, R. E., Vladimirou, E., & Janes, S. M. (2018). The secret lives of cancer cell lines. *DMM Disease Models and Mechanisms*, *11*(11). https://doi.org/10.1242/dmm.037366

Imbault, M., Chauvet, D., Gennisson, J. L., Capelle, L., & Tanter, M. (2017). Intraoperative Functional Ultrasound Imaging of Human Brain Activity. *Scientific Reports*, *7*(1). https://doi.org/10.1038/s41598-017-06474-8

Israeli-Rosenberg, S., Manso, A. M., Okada, H., & Ross, R. S. (2014). Integrins and integrin-associated proteins in the cardiac myocyte. In *Circulation Research* (Vol. 114, Issue 3). https://doi.org/10.1161/CIRCRESAHA.114.301275

Iwadate, Y. (2016). Epithelial-mesenchymal transition in glioblastoma progression. In *Oncology Letters* (Vol. 11, Issue 3). https://doi.org/10.3892/ol.2016.4113

Iwamoto, D. V., & Calderwood, D. A. (2015). Regulation of integrin-mediated adhesions. In *Current Opinion in Cell Biology* (Vol. 36). https://doi.org/10.1016/j.ceb.2015.06.009

Jafari, A., Hassanajili, S., Ghaffari, F., & Azarpira, N. (2022). Modulating the physico-mechanical properties of polyacrylamide/gelatin hydrogels for tissue engineering application. *Polymer Bulletin*, *79*(3). https://doi.org/10.1007/s00289-021-03592-2

Joyce, T., Jagasia, S., Tasci, E., Camphausen, K., & Krauze, A. V. (2023). An Overview of CD133 as a Functional Unit of Prognosis and Treatment Resistance in Glioblastoma. In *Current Oncology* (Vol. 30, Issue 9). https://doi.org/10.3390/curroncol30090601

Kalluri, R. (2009). EMT: When epithelial cells decide to become mesenchymal-like cells. In *Journal of Clinical Investigation* (Vol. 119, Issue 6). https://doi.org/10.1172/JCI39675

Kalluri, R., & Weinberg, R. A. (2009). The basics of epithelial-mesenchymal transition. In *Journal of Clinical Investigation* (Vol. 119, Issue 6). https://doi.org/10.1172/JCI39104

Kandow, C. E., Georges, P. C., Janmey, P. A., & Beningo, K. A. (2007). Polyacrylamide Hydrogels for Cell Mechanics: Steps Toward Optimization and Alternative Uses. In *Methods in Cell Biology* (Vol. 83). https://doi.org/10.1016/S0091-679X(07)83002-0

Kapałczyńska, M., Kolenda, T., Przybyła, W., Zajączkowska, M., Teresiak, A., Filas, V., Ibbs, M., Bliźniak, R., Łuczewski, Ł., & Lamperska, K. (2018). 2D and 3D cell cultures – a comparison of different types of cancer cell

cultures. *Archives of Medical Science*, *14*(4). https://doi.org/10.5114/aoms.2016.63743

Kaunas, R., Nguyen, P., Usami, S., & Chien, S. (2005). Cooperative effects of Rho and mechanical stretch on stress fiber organization. *Proceedings of the National Academy of Sciences of the United States of America*, *102*(44). https://doi.org/10.1073/pnas.0506041102

Kim, D. H., Provenzano, P. P., Smith, C. L., & Levchenko, A. (2012). Matrix nanotopography as a regulator of cell function. In *Journal of Cell Biology* (Vol. 197, Issue 3). https://doi.org/10.1083/jcb.201108062

Kim, J., Darlington, A., Salvador, M., Utrilla, J., & Jiménez, J. I. (2020). Trade-offs between gene expression, growth and phenotypic diversity in microbial populations. In *Current Opinion in Biotechnology* (Vol. 62). https://doi.org/10.1016/j.copbio.2019.08.004

Kim, S. N., Jeibmann, A., Halama, K., Witte, H. T., Wälte, M., Matzat, T., Schillers, H., Faber, C., Senner, V., Paulus, W., & Klämbt, C. (2014). ECM stiffness regulates glial migration in Drosophila and mammalian glioma models. *Development (Cambridge)*, *141*(16). https://doi.org/10.1242/dev.106039

Kim, Y. E., Won, M., Lee, S. G., Park, C., Song, C. H., & Kim, K. K. (2019). RBM47-regulated alternative splicing of TJP1 promotes actin stress fiber assembly during epithelial-to-mesenchymal transition. *Oncogene*, *38*(38). https://doi.org/10.1038/s41388-019-0892-5

Kim, Y., & Kumar, S. (2014). CD44-mediated adhesion to hyaluronic acid contributes to mechanosensing and invasive motility. *Molecular Cancer Research*, *12*(10). https://doi.org/10.1158/1541-7786.MCR-13-0629

Krishnamurthy, S., & Nör, J. E. (2013). Orosphere assay: A method for propagation of head and neck cancer stem cells. *Head and Neck*, *35*(7). https://doi.org/10.1002/hed.23076

Kröger, C., Afeyan, A., Mraz, J., Eaton, E. N., Reinhardt, F., Khodor, Y. L., Thiru, P., Bierie, B., Ye, X., Burge, C. B., & Weinberg, R. A. (2019). Acquisition of a hybrid E/M state is essential for tumorigenicity of basal breast cancer cells. *Proceedings of the National Academy of Sciences of the United States of America*, *116*(15). https://doi.org/10.1073/pnas.1812876116

Lamouille, S., Xu, J., & Derynck, R. (2014). Molecular mechanisms of epithelial-mesenchymal transition. In *Nature Reviews Molecular Cell Biology* (Vol. 15, Issue 3). https://doi.org/10.1038/nrm3758

Lee, J., Abdeen, A. A., Zhang, D., & Kilian, K. A. (2013). Directing stem cell fate on hydrogel substrates by controlling cell geometry, matrix mechanics and adhesion ligand composition. *Biomaterials*, *34*(33). https://doi.org/10.1016/j.biomaterials.2013.07.074

Lee, J., Cuddihy, M. J., & Kotov, N. A. (2008). Three-dimensional cell culture matrices: State of the art. In *Tissue Engineering - Part B: Reviews* (Vol. 14, Issue 1). https://doi.org/10.1089/teb.2007.0150

Lee, J. P., Kassianidou, E., MacDonald, J. I., Francis, M. B., & Kumar, S. (2016). N-terminal specific conjugation of extracellular matrix proteins to 2-pyridinecarboxaldehyde functionalized polyacrylamide hydrogels. *Biomaterials*, *102*. https://doi.org/10.1016/j.biomaterials.2016.06.022

Leggett, S. E., Hruska, A. M., Guo, M., & Wong, I. Y. (2021). The epithelial-mesenchymal transition and the cytoskeleton in bioengineered systems. In *Cell Communication and Signaling* (Vol. 19, Issue 1). https://doi.org/10.1186/s12964-021-00713-2

Levental, K. R., Yu, H., Kass, L., Lakins, J. N., Egeblad, M., Erler, J. T., Fong, S. F. T., Csiszar, K., Giaccia, A., Weninger, W., Yamauchi, M., Gasser, D. L., & Weaver, V. M. (2009). Matrix Crosslinking Forces Tumor Progression by Enhancing Integrin Signaling. *Cell*, *139*(5). https://doi.org/10.1016/j.cell.2009.10.027

Lewis-Tuffin, L. J., Rodriguez, F., Giannini, C., Scheithauer, B., Necela, B. M., Sarkaria, J. N., & Anastasiadis, P. Z. (2010). Misregulated E-Cadherin expression associated with an aggressive brain tumor phenotype. *PLoS ONE*, *5*(10). https://doi.org/10.1371/journal.pone.0013665

Li, M., Wang, Y., Li, M., Wu, X., Setrerrahmane, S., & Xu, H. (2021). Integrins as attractive targets for cancer therapeutics. In *Acta Pharmaceutica Sinica B* (Vol. 11, Issue 9). https://doi.org/10.1016/j.apsb.2021.01.004

Li, T., Guo, H., Song, Y., Zhao, X., Shi, Y., Lu, Y., Hu, S., Nie, Y., Fan, D., & Wu, K. (2014). Loss of vinculin and membrane-bound β-catenin promotes metastasis and predicts poor prognosis in colorectal cancer. *Molecular Cancer*, *13*(1). https://doi.org/10.1186/1476-4598-13-263

Li, Y., Wang, Z., Ajani, J. A., & Song, S. (2021). Drug resistance and Cancer stem cells. In *Cell Communication and Signaling* (Vol. 19, Issue 1). https://doi.org/10.1186/s12964-020-00627-5

Liu, R., Wang, X., Chen, G. Y., Dalerba, P., Gurney, A., Hoey, T., Sherlock, G., Lewicki, J., Shedden, K., & Clarke, M. F. (2007). The Prognostic Role of a Gene Signature from Tumorigenic Breast-Cancer Cells. *New England Journal of Medicine*, *356*(3). https://doi.org/10.1056/nejmoa063994

Lu, W., & Kang, Y. (2019). Epithelial-Mesenchymal Plasticity in Cancer Progression and Metastasis. In *Developmental Cell* (Vol. 49, Issue 3). https://doi.org/10.1016/j.devcel.2019.04.010

Luo, J., Walker, M., Xiao, Y., Donnelly, H., Dalby, M. J., & Salmeron-Sanchez, M. (2022). The influence of nanotopography on cell behaviour through interactions with the extracellular matrix – A review. In *Bioactive Materials* (Vol. 15). https://doi.org/10.1016/j.bioactmat.2021.11.024

Ma, T., Hu, C., Lal, B., Zhou, W., Ma, Y., Ying, M., Prinos, P., Quiñones-Hinojosa, A., Lim, M., Laterra, J., & Li, Y. (2021). Reprogramming transcription factors Oct4 and Sox2 induce a BRD-dependent immunosuppressive transcriptome in GBM-propagating cells. *Cancer Research*, *81*(9). https://doi.org/10.1158/0008-5472.CAN-20-2489

Maekawa, M., Ishizaki, T., Boku, S., Watanabe, N., Fujita, A., Iwamatsu, A., Obinata, T., Ohashi, K., Mizuno, K., & Narumiya, S. (1999). Signaling from Rho to the actin cytoskeleton through protein kinases ROCK and LIM-kinase. *Science*, *285*(5429). https://doi.org/10.1126/science.285.5429.895

Maher, E. A., Furnari, F. B., Bachoo, R. M., Rowitch, D. H., Louis, D. N., Cavenee, W. K., & DePinho, R. A. (2001). Malignant glioma: Genetics and biology of a grave matter. In *Genes and Development* (Vol. 15, Issue 11). https://doi.org/10.1101/gad.891601

Mahesparan, R., Read, T. A., Lund-Johansen, M., Skaftnesmo, K. O., Bjerkvig, R., & Engebraaten, O. (2003). Expression of extracellular matrix components in a highly infiltrative in vivo glioma model. *Acta Neuropathologica*, *105*(1). https://doi.org/10.1007/s00401-002-0610-0

Mani, S. A., Guo, W., Liao, M. J., Eaton, E. N., Ayyanan, A., Zhou, A. Y., Brooks, M., Reinhard, F., Zhang, C. C., Shipitsin, M., Campbell, L. L., Polyak, K., Brisken, C., Yang, J., & Weinberg, R. A. (2008). The Epithelial-Mesenchymal Transition Generates Cells with Properties of Stem Cells. *Cell*, *133*(4). https://doi.org/10.1016/j.cell.2008.03.027

Matte, B. F., Kumar, A., Placone, J. K., Zanella, V. G., Martins, M. D., Engler, A. J., & Lamers, M. L. (2019). Matrix stiffness mechanically conditions EMT and migratory behavior of oral squamous cell carcinoma. In *Journal of Cell Science* (Vol. 132, Issue 1). https://doi.org/10.1242/jcs.224360

May, C. D., Sphyris, N., Evans, K. W., Werden, S. J., Guo, W., & Mani, S. A. (2011). Epithelial-mesenchymal transition and cancer stem cells: A dangerously dynamic duo in breast cancer progression. In *Breast Cancer Research* (Vol. 13, Issue 1). https://doi.org/10.1186/bcr2789

Mazzoleni, G., Di Lorenzo, D., & Steimberg, N. (2009). Modelling tissues in 3D: The next future of pharmaco-toxicology and food research? In *Genes and Nutrition* (Vol. 4, Issue 1). https://doi.org/10.1007/s12263-008-0107-0

McBeath, R., Pirone, D. M., Nelson, C. M., Bhadriraju, K., & Chen, C. S. (2004). Cell shape, cytoskeletal tension, and RhoA regulate stem cell lineage commitment. *Developmental Cell*, *6*(4). https://doi.org/10.1016/S1534-5807(04)00075-9

McDermott, S. P., & Wicha, M. S. (2010). Targeting breast cancer stem cells. In *Molecular Oncology* (Vol. 4, Issue 5). https://doi.org/10.1016/j.molonc.2010.06.005

McNamara, C., Mankad, K., Thust, S., Dixon, L., Limback-Stanic, C., D'Arco, F., Jacques, T. S., & Löbel, U. (2022). 2021 WHO classification of tumours of the central nervous system: a review for the neuroradiologist. *Neuroradiology*, *64*(10), 1919–1950.

Meacham, C. E., & Morrison, S. J. (2013). Tumour heterogeneity and cancer cell plasticity. In *Nature* (Vol. 501, Issue 7467). https://doi.org/10.1038/nature12624

Melissaridou, S., Wiechec, E., Magan, M., Jain, M. V., Chung, M. K., Farnebo, L., & Roberg, K. (2019). The effect of 2D and 3D cell cultures on treatment response, EMT profile and stem cell features in head and neck cancer. *Cancer Cell International*, *19*(1). https://doi.org/10.1186/s12935-019-0733-1

Mia-Jan, K., Jung, S. Y., Kim, I. Y., Oh, S. S., Choi, E. H., Chang, S. J., Kang, T. Y., & Cho, M. Y. (2013). CD133 expression is not an independent prognostic factor in stage II and III colorectal cancer but may predict the better outcome in patients with adjuvant therapy. *BMC Cancer*, *13*. https://doi.org/10.1186/1471-2407-13-166

Micalizzi, D. S., Farabaugh, S. M., & Ford, H. L. (2010). Epithelial-mesenchymal transition in cancer: Parallels between normal development and tumor progression. In *Journal of Mammary Gland Biology and Neoplasia* (Vol. 15, Issue 2). https://doi.org/10.1007/s10911-010-9178-9

Mikheeva, S. A., Mikheev, A. M., Petit, A., Beyer, R., Oxford, R. G., Khorasani, L., Maxwell, J. P., Glackin, C. A., Wakimoto, H., González-Herrero, I., Sánchez-García, I., Silber, J. R., Horner, P. J., & Rostomily, R. C. (2010). TWIST1 promotes invasion through mesenchymal change in human glioblastoma. *Molecular Cancer*, *9*. https://doi.org/10.1186/1476-4598-9-194

Miroshnikova, Y. A., Mouw, J. K., Barnes, J. M., Pickup, M. W., Lakins, J. N., Kim, Y., Lobo, K., Persson, A. I., Reis, G. F., McKnigh, T. R., Holland, E. C., Phillips, J. J., & Weaver, V. M. (2016). Tissue mechanics promote IDH1-dependent HIF1α-tenascin C feedback to regulate glioblastoma aggression. *Nature Cell Biology*, *18*(12). https://doi.org/10.1038/ncb3429

Mohiuddin, E., & Wakimoto, H. (2021). Extracellular matrix in glioblastoma: opportunities for emerging therapeutic approaches. *American Journal of Cancer Research*, *11*(8).

Monzo, P., Crestani, M., Chong, Y. K., Ghisleni, A., Hennig, K., Li, Q., Kakogiannos, N., Giannotta, M., Richichi, C., Dini, T., Dejana, E., Maiuri, P., Balland, M., Sheetz, M. P., Pelicci, G., Ang, B. T., Tang, C., & Gauthier, N. C. (2021). Adaptive mechanoproperties mediated by the formin FMN1 characterize glioblastoma fitness for invasion. *Developmental Cell*, *56*(20). https://doi.org/10.1016/j.devcel.2021.09.007

Mouw, J. K., Yui, Y., Damiano, L., Bainer, R. O., Lakins, J. N., Acerbi, I., Ou, G., Wijekoon, A. C., Levental, K. R., Gilbert, P. M., Hwang, E. S., Chen, Y. Y., & Weaver, V. M. (2014). Tissue mechanics modulate microRNA-dependent PTEN expression to regulate malignant progression. *Nature Medicine*, *20*(4). https://doi.org/10.1038/nm.3497

Nagaishi, M., Paulus, W., Brokinkel, B., Vital, A., Tanaka, Y., Nakazato, Y., Giangaspero, F., & Ohgaki, H. (2012). Transcriptional factors for epithelial-mesenchymal transition are associated with mesenchymal differentiation in gliosarcoma. *Brain Pathology*, *22*(5). https://doi.org/10.1111/j.1750-3639.2012.00571.x

Nelson, C. M., Khauv, D., Bissell, M. J., & Radisky, D. C. (2008). Change in cell shape is required for matrix metalloproteinase-induced epithelial-mesenchymal transition of mammary epithelial cells. *Journal of Cellular Biochemistry*, *105*(1). https://doi.org/10.1002/jcb.21821

Neradil, J., & Veselska, R. (2015). Nestin as a marker of cancer stem cells. In *Cancer Science* (Vol. 106, Issue 7). https://doi.org/10.1111/cas.12691

Nieto, M. A., Huang, R. Y. Y. J., Jackson, R. A. A., & Thiery, J. P. P. (2016). EMT: 2016. In *Cell* (Vol. 166, Issue 1). https://doi.org/10.1016/j.cell.2016.06.028

Noronha, C., Ribeiro, A. S., Taipa, R., Castro, D. S., Reis, J., Faria, C., & Paredes, J. (2021). Cadherin expression and emt: A focus on gliomas. In *Biomedicines* (Vol. 9, Issue 10). https://doi.org/10.3390/biomedicines9101328

Ocaña, O. H., Córcoles, R., Fabra, Á., Moreno-Bueno, G., Acloque, H., Vega, S., Barrallo-Gimeno, A., Cano, A., & Nieto, M. A. (2012). Metastatic Colonization Requires the Repression of the Epithelial-Mesenchymal Transition Inducer Prrx1. *Cancer Cell*, *22*(6). https://doi.org/10.1016/j.ccr.2012.10.012

Oh, M., Batty, S., Banerjee, N., & Kim, T. H. (2023). High extracellular glucose promotes cell motility by modulating cell deformability and contractility via the cAMP-RhoA-ROCK axis in human breast cancer cells. *Molecular Biology of the Cell*, *34*(8). https://doi.org/10.1091/mbc.E22-12-0560

Ohashi, K., Fujiwara, S., & Mizuno, K. (2017). Roles of the cytoskeleton, cell adhesion and rho signalling in mechanosensing and mechanotransduction. In *Journal of Biochemistry* (Vol. 161, Issue 3). https://doi.org/10.1093/jb/mvw082

Oprita, A., Baloi, S. C., Staicu, G. A., Alexandru, O., Tache, D. E., Danoiu, S., Micu, E. S., & Sevastre, A. S. (2021). Updated insights on EGFR signaling pathways in glioma. In *International Journal of Molecular Sciences* (Vol. 22, Issue 2). https://doi.org/10.3390/ijms22020587

Ostrom, Q. T., Gittleman, H., Fulop, J., Liu, M., Blanda, R., Kromer, C., Wolinsky, Y., Kruchko, C., & Barnholtz-Sloan, J. S. (2015). CBTRUS statistical Report: primary brain and central nervous system tumors

diagnosed in the United States in 2008-2012. *Neuro-Oncology*, *17*. https://doi.org/10.1093/neuonc/nov189

Pampaloni, F., Reynaud, E. G., & Stelzer, E. H. K. (2007). The third dimension bridges the gap between cell culture and live tissue. In *Nature Reviews Molecular Cell Biology* (Vol. 8, Issue 10). https://doi.org/10.1038/nrm2236

Park, J., & Schwarzbauer, J. E. (2014). Mammary epithelial cell interactions with fibronectin stimulate epithelial-mesenchymal transition. *Oncogene*, *33*(13). https://doi.org/10.1038/onc.2013.118

Paszek, M. J., Zahir, N., Johnson, K. R., Lakins, J. N., Rozenberg, G. I., Gefen, A., Reinhart-King, C. A., Margulies, S. S., Dembo, M., Boettiger, D., Hammer, D. A., & Weaver, V. M. (2005). Tensional homeostasis and the malignant phenotype. *Cancer Cell*, *8*(3). https://doi.org/10.1016/j.ccr.2005.08.010

Paul, I., Bhattacharya, S., Chatterjee, A., & Ghosh, M. K. (2013). Current Understanding on EGFR and Wnt/β-Catenin Signaling in Glioma and Their Possible Crosstalk. In *Genes and Cancer* (Vol. 4, Issues 11–12). https://doi.org/10.1177/1947601913503341

Payne, L. S., & Huang, P. H. (2013). The pathobiology of collagens in glioma. In *Molecular Cancer Research* (Vol. 11, Issue 10). https://doi.org/10.1158/1541-7786.MCR-13-0236

Phillips, H. S., Kharbanda, S., Chen, R., Forrest, W. F., Soriano, R. H., Wu, T. D., Misra, A., Nigro, J. M., Colman, H., Soroceanu, L., Williams, P. M., Modrusan, Z., Feuerstein, B. G., & Aldape, K. (2006). Molecular subclasses of high-grade glioma predict prognosis, delineate a pattern of disease progression, and resemble stages in neurogenesis. *Cancer Cell*, *9*(3). https://doi.org/10.1016/j.ccr.2006.02.019

Pogoda, K., Chin, L., Georges, P. C., Byfield, F. J., Bucki, R., Kim, R., Weaver, M., Wells, R. G., Marcinkiewicz, C., & Janmey, P. A. (2014). Compression stiffening of brain and its effect on mechanosensing by glioma cells. *New Journal of Physics*, *16*. https://doi.org/10.1088/1367-2630/16/7/075002

Pollak, N., Lindner, A., Imig, D., Kuritz, K., Fritze, J. S., Decker, L., Heinrich, I., Stadager, J., Eisler, S., Stöhr, D., Allgöwer, F., Scheurich, P., & Rehm, M. (2021). Cell cycle progression and transmitotic apoptosis resistance promote escape from extrinsic apoptosis. *Journal of Cell Science*, *134*(24). https://doi.org/10.1242/jcs.258966

Poonaki, E., Kahlert, U. D., Meuth, S. G., & Gorji, A. (2022). The role of the ZEB1–neuroinflammation axis in CNS disorders. In *Journal of Neuroinflammation* (Vol. 19, Issue 1). https://doi.org/10.1186/s12974-022-02636-2

Pors, K., & Moreb, J. S. (2014). Aldehyde dehydrogenases in cancer: An opportunity for biomarker and drug development? In *Drug Discovery Today* (Vol. 19, Issue 12). https://doi.org/10.1016/j.drudis.2014.09.009

Qi, S., Song, Y., Peng, Y., Wang, H., Long, H., Yu, X., Li, Z., Fang, L., Wu, A., Luo, W., Zhen, Y., Zhou, Y., Chen, Y., Mai, C., Liu, Z., & Fang, W. (2012). ZEB2 mediates multiple pathways regulating cell proliferation, migration, invasion, and apoptosis in glioma. *PLoS ONE*, *7*(6). https://doi.org/10.1371/journal.pone.0038842

Qiao, Y. N., He, W. Q., Chen, C. P., Zhang, C. H., Zhao, W., Wang, P., Zhang, L., Wu, Y. Z., Yang, X., Peng, Y. J., Gao, J. M., Kamm, K. E., Stull, J. T., & Zhu, M. S. (2014). Myosin phosphatase target subunit 1 (MYPT1) regulates the contraction and relaxation of vascular smooth muscle and maintains

blood pressure. *Journal of Biological Chemistry*, *289*(32). https://doi.org/10.1074/jbc.M113.525444

Raguž, M., Tarle, M., Müller, D., Tomasović-Lončarić, Č., Chudy, H., Marinović, T., & Chudy, D. (2024). ABCG2 Expression as a Potential Survival Predictor in Human Gliomas. *International Journal of Molecular Sciences*, *25*(6). https://doi.org/10.3390/ijms25063116

Raha, D., Wilson, T. R., Peng, J., Peterson, D., Yue, P., Evangelista, M., Wilson, C., Merchant, M., & Settleman, J. (2014). The cancer stem cell marker aldehyde dehydrogenase is required to maintain a drug-tolerant tumor cell subpopulation. *Cancer Research*, *74*(13). https://doi.org/10.1158/0008-5472.CAN-13-3456

Riento, K., & Ridley, A. J. (2003). Rocks: Multifunctional kinases in cell behaviour. In *Nature Reviews Molecular Cell Biology* (Vol. 4, Issue 6). https://doi.org/10.1038/nrm1128

Ruiz-Ontañon, P., Orgaz, J. L., Aldaz, B., Elosegui-Artola, A., Martino, J., Berciano, M. T., Montero, J. A., Grande, L., Nogueira, L., Diaz-Moralli, S., Esparís-Ogando, A., Vazquez-Barquero, A., Lafarga, M., Pandiella, A., Cascante, M., Segura, V., Martinez-Climent, J. A., Sanz-Moreno, V., & Fernandez-Luna, J. L. (2013). Cellular plasticity confers migratory and invasive advantages to a population of glioblastoma-initiating cells that infiltrate peritumoral tissue. *Stem Cells*, *31*(6). https://doi.org/10.1002/stem.1349

Sánchez-Tilló, E., Liu, Y., De Barrios, O., Siles, L., Fanlo, L., Cuatrecasas, M., Darling, D. S., Dean, D. C., Castells, A., & Postigo, A. (2012). EMT-activating transcription factors in cancer: Beyond EMT and tumor invasiveness. In *Cellular and Molecular Life Sciences* (Vol. 69, Issue 20). https://doi.org/10.1007/s00018-012-1122-2

Scheel, C., & Weinberg, R. A. (2012). Cancer stem cells and epithelial-mesenchymal transition: Concepts and molecular links. In *Seminars in Cancer Biology* (Vol. 22, Issues 5–6). https://doi.org/10.1016/j.semcancer.2012.04.001

Shafi, O., & Siddiqui, G. (2022). Tracing the origins of glioblastoma by investigating the role of gliogenic and related neurogenic genes/signaling pathways in GBM development: a systematic review. *World Journal of Surgical Oncology*, *20*(1). https://doi.org/10.1186/s12957-022-02602-5

Sheridan, C., Kishimoto, H., Fuchs, R. K., Mehrotra, S., Bhat-Nakshatri, P., Turner, C. H., Goulet, R., Badve, S., & Nakshatri, H. (2006). CD44+/CD24- Breast cancer cells exhibit enhanced invase properties: An early step necessary for metastasis. *Breast Cancer Research*, *8*(5). https://doi.org/10.1186/bcr1610

Sin, W.-C., Chen, X.-Q., Leung, T., & Lim, L. (1998). RhoA-Binding Kinase α Translocation Is Facilitated by the Collapse of the Vimentin Intermediate Filament Network. *Molecular and Cellular Biology*, *18*(11). https://doi.org/10.1128/mcb.18.11.6325

Singh, S. K., Clarke, I. D., Terasaki, M., Bonn, V. E., Hawkins, C., Squire, J., & Dirks, P. B. (2003). Identification of a cancer stem cell in human brain tumors. *Cancer Research*, *63*(18).

Sohrabi, A., Lefebvre, A. E. Y. T., Harrison, M. J., Condro, M. C., Sanazzaro, T. M., Safarians, G., Solomon, I., Bastola, S., Kordbacheh, S., Toh, N., Kornblum, H. I., Digman, M. A., & Seidlits, S. K. (2023). Microenvironmental stiffness induces metabolic reprogramming in glioblastoma. *Cell Reports*, *42*(10). https://doi.org/10.1016/j.celrep.2023.113175

Stanton, A. E., Tong, X., Lee, S., & Yang, F. (2019). Biochemical Ligand Density Regulates Yes-Associated Protein Translocation in Stem Cells through Cytoskeletal Tension and Integrins. *ACS Applied Materials and Interfaces*, *11*(9). https://doi.org/10.1021/acsami.8b21270

Steinbichler, T. B., Dudás, J., Skvortsov, S., Ganswindt, U., Riechelmann, H., & Skvortsova, I. I. (2018). Therapy resistance mediated by cancer stem cells. In *Seminars in Cancer Biology* (Vol. 53). https://doi.org/10.1016/j.semcancer.2018.11.006

Storms, R. W., Trujillo, A. P., Springer, J. B., Shah, L., Colvin, O. M., Ludeman, S. M., & Smith, C. (1999). Isolation of primitive human hematopoietic progenitors on the basis of aldehyde dehydrogenase activity. *Proceedings of the National Academy of Sciences of the United States of America*, *96*(16). https://doi.org/10.1073/pnas.96.16.9118

Strojnik, T., Røsland, G. V., Sakariassen, P. O., Kavalar, R., & Lah, T. (2007). Neural stem cell markers, nestin and musashi proteins, in the progression of human glioma: correlation of nestin with prognosis of patient survival. *Surgical Neurology*, *68*(2). https://doi.org/10.1016/j.surneu.2006.10.050

Stupp, R., Hegi, M. E., Mason, W. P., van den Bent, M. J., Taphoorn, M. J., Janzer, R. C., Ludwin, S. K., Allgeier, A., Fisher, B., Belanger, K., Hau, P., Brandes, A. A., Gijtenbeek, J., Marosi, C., Vecht, C. J., Mokhtari, K., Wesseling, P., Villa, S., Eisenhauer, E., … Mirimanoff, R. O. (2009). Effects of radiotherapy with concomitant and adjuvant temozolomide versus radiotherapy alone on survival in glioblastoma in a randomised phase III study: 5-year analysis of the EORTC-NCIC trial. *The Lancet Oncology*, *10*(5). https://doi.org/10.1016/S1470-2045(09)70025-7

Sun, Z., Guo, S. S., & Fässler, R. (2016). Integrin-mediated mechanotransduction. In *Journal of Cell Biology* (Vol. 215, Issue 4). https://doi.org/10.1083/jcb.201609037

Their, J. P. (2002). Epithelial-mesenchymal transitions in tumor progression. In *Nature Reviews Cancer* (Vol. 2, Issue 6). https://doi.org/10.1038/nrc822

Thiery, J. P., Acloque, H., Huang, R. Y. J., & Nieto, M. A. (2009). Epithelial-Mesenchymal Transitions in Development and Disease. In *Cell* (Vol. 139, Issue 5). https://doi.org/10.1016/j.cell.2009.11.007

Thorén, M. M., Masoumi, K. C., Krona, C., Huang, X., Kundu, S., Schmidt, L., Forsberg-Nilsson, K., Keep, M. F., Englund, E., Nelander, S., Holmqvist, B., & Lundgren-Åkerlund, E. (2019). Integrin α10, a novel therapeutic target in glioblastoma, regulates cell migration, proliferation, and survival. *Cancers*, *11*(4). https://doi.org/10.3390/cancers11040587

Torsvik, A., Stieber, D., Enger, P. O., Golebiewska, A., Molven, A., Svendsen, A., Westermark, B., Niclou, S. P., Olsen, T. K., Chekenya Enger, M., & Bjerkvig, R. (2014). U-251 revisited: Genetic drift and phenotypic consequences of long-term cultures of glioblastoma cells. *Cancer Medicine*, *3*(4). https://doi.org/10.1002/cam4.219

Totsukawa, G., Yamakita, Y., Yamashiro, S., Hartshorne, D. J., Sasaki, Y., & Matsumura, F. (2000). Distinct roles of ROCK (Rho-kinase) and MLCK in spatial regulation of MLC phosphorylation for assembly of stress fibers and focal adhesions in 3T3 fibroblasts. *Journal of Cell Biology*, *150*(4). https://doi.org/10.1083/jcb.150.4.797

Ulrich, T. A., De Juan Pardo, E. M., & Kumar, S. (2009). The mechanical rigidity of the extracellular matrix regulates the structure, motility, and proliferation of glioma cells. *Cancer Research*, *69*(10). https://doi.org/10.1158/0008-5472.CAN-08-4859

Verhaak, R. G. W., Hoadley, K. A., Purdom, E., Wang, V., Qi, Y., Wilkerson, M. D., Miller, C. R., Ding, L., Golub, T., Mesirov, J. P., Alexe, G., Lawrence, M., O'Kelly, M., Tamayo, P., Weir, B. A., Gabriel, S., Winckler, W., Gupta, S., Jakkula, L., … Hayes, D. N. (2010). Integrated Genomic Analysis Identifies Clinically Relevant Subtypes of Glioblastoma Characterized by Abnormalities in PDGFRA, IDH1, EGFR, and NF1. *Cancer Cell*, *17*(1). https://doi.org/10.1016/j.ccr.2009.12.020

Wang, H., Wang, S., Hu, J., Kong, Y., Chen, S., Li, L., & Li, L. (2009). Oct4 is expressed in Nestin-positive cells as a marker for pancreatic endocrine progenitor. *Histochemistry and Cell Biology*, *131*(5). https://doi.org/10.1007/s00418-009-0560-x

Wang, J. H. C. (2006). Mechanobiology of tendon. In *Journal of Biomechanics* (Vol. 39, Issue 9). https://doi.org/10.1016/j.jbiomech.2005.05.011

Wang, Q., Li, X., Zhu, Y., & Yang, P. (2014). MicroRNA-16 suppresses epithelial-mesenchymal transition-related gene expression in human glioma. *Molecular Medicine Reports*, *10*(6). https://doi.org/10.3892/mmr.2014.2583

Wang, Q., Wu, H., Hu, J., Fu, H., Qu, Y., Yang, Y., Cai, Q., Efimov, A., Wu, M., Yen, T., Wang, Y., & Yang, Z. J. (2021). Nestin is required for spindle assembly and cell cycle progression in glioblastoma cells. *Molecular Cancer Research*, *19*(10). https://doi.org/10.1158/1541-7786.MCR-20-0994

Wang, Y. L., & Pelham, R. J. (1998). [39] Preparation of a flexible, porous polyacrylamide substrate for mechanical studies of cultured cells. *Methods in Enzymology*, *298*. https://doi.org/10.1016/S0076-6879(98)98041-7

Wong, S. Y., Ulrich, T. A., Deleyrolle, L. P., MacKay, J. L., Lin, J. M. G., Martuscello, R. T., Jundi, M. A., Reynolds, B. A., & Kumar, S. (2015). Constitutive activation of myosin-dependent contractility sensitizes glioma tumor-initiating cells to mechanical inputs and reduces tissue invasion. *Cancer Research*, *75*(6). https://doi.org/10.1158/0008-5472.CAN-13-3426

Wu, Y., Kram, H., Gempt, J., Liesche-Starnecker, F., Wu, W., & Schlegel, J. (2022). ALDH1-Mediated Autophagy Sensitizes Glioblastoma Cells to Ferroptosis. *Cells*, *11*(24). https://doi.org/10.3390/cells11244015

Würth, R., Bajetto, A., Harrison, J. K., Barbieri, F., & Florio, T. (2014). CXCL12 modulation of CXCR4 and CXCR7 activity in human glioblastoma stem-like cells and regulation of the tumor microenvironment. In *Frontiers in Cellular Neuroscience* (Vol. 8, Issue MAY). https://doi.org/10.3389/fncel.2014.00144

Xie, Y. K., Huo, S. F., Zhang, G., Zhang, F., Lian, Z. P., Tang, X. L., & Jin, C. (2012). CDA-2 induces cell differentiation through suppressing Twist/SLUG signaling via miR-124 in glioma. *Journal of Neuro-Oncology*, *110*(2). https://doi.org/10.1007/s11060-012-0961-x

Xu, J., Lamouille, S., & Derynck, R. (2009). TGF-B-induced epithelial to mesenchymal transition. In *Cell Research* (Vol. 19, Issue 2). https://doi.org/10.1038/cr.2009.5

Xu, J., Sun, M., Tan, Y., Wang, H., Wang, H., Li, P., Xu, Z., Xia, Y., Li, L., & Li, Y. (2017). Effect of matrix stiffness on the proliferation and differentiation of umbilical cord mesenchymal stem cells. *Differentiation*, *96*. https://doi.org/10.1016/j.diff.2017.07.001

Yang, H. W., Menon, L. G., Black, P. M., Carroll, R. S., & Johnson, M. D. (2010). SNAI2/Slug promotes growth and invasion in human gliomas. *BMC Cancer*, *10*. https://doi.org/10.1186/1471-2407-10-301

Yang, M. H., Wu, M. Z., Chiou, S. H., Chen, P. M., Chang, S. Y., Liu, C. J., Teng, S. C., & Wu, K. J. (2008). Direct regulation of TWIST by HIF-1α promotes metastasis. *Nature Cell Biology*, *10*(3). https://doi.org/10.1038/ncb1691

Yang, Y. H. K., Ogando, C. R., Wang See, C., Chang, T. Y., & Barabino, G. A. (2018). Changes in phenotype and differentiation potential of human mesenchymal stem cells aging in vitro. *Stem Cell Research and Therapy*, *9*(1). https://doi.org/10.1186/s13287-018-0876-3

Yiming, L., Yunshan, G., Bo, M., Yu, Z., Tao, W., Gengfang, L., Dexian, F., Shiqian, C., Jianli, J., Juan, T., & Zhinan, C. (2015). CD133 overexpression correlates with clinicopathological features of gastric cancer patients and its impact on survival: A systematic review and meta-analysis. *Oncotarget*, *6*(39). https://doi.org/10.18632/oncotarget.5714

Yue, H., Hu, Z., Hu, R., Guo, Z., Zheng, Y., Wang, Y., & Zhou, Y. (2022). ALDH1A1 in Cancers: Bidirectional Function, Drug Resistance, and Regulatory Mechanism. In *Frontiers in Oncology* (Vol. 12). https://doi.org/10.3389/fonc.2022.918778

Yui, A., & Oudin, M. J. (2024). The Rigidity Connection: Matrix Stiffness and Its Impact on Cancer Progression. *Cancer Research*, *84*(7), 958–960.

Zeisberg, M., & Neilson, E. G. (2009). Biomarkers for epithelial-mesenchymal transitions. In *Journal of Clinical Investigation* (Vol. 119, Issue 6). https://doi.org/10.1172/JCI36183

Zenzmaier, C., Untergasser, G., & Berger, P. (2008). Aging of the prostate epithelial stem/progenitor cell. In *Experimental Gerontology* (Vol. 43, Issue 11). https://doi.org/10.1016/j.exger.2008.06.008

Zhong, C., Tao, B., Tang, F., Yang, X., Peng, T., You, J., Xia, K., Xia, X., Chen, L., & Peng, L. (2021). Remodeling cancer stemness by collagen/fibronectin via the AKT and CDC42 signaling pathway crosstalk in glioma. *Theranostics*, *11*(4). https://doi.org/10.7150/thno.50613